

Circumstellar interaction in supernovae in dense environments - an observational perspective

Poonam Chandra^{1,2}

Received: date / Accepted: date

Abstract In a supernova explosion, the ejecta interacting with the surrounding circumstellar medium (CSM) give rise to variety of radiation. Since CSM is created from the mass lost from the progenitor star, it carries foot prints of the late time evolution of the star. This is one of the unique ways to get a handle on the nature of the progenitor star system. Here, I will focus mainly on the supernovae (SNe) exploding in dense environments, a.k.a. Type IIn SNe. Radio and X-ray emission from this class of SNe have revealed important modifications in their radiation properties, due to the presence of high density CSM. Forward shock dominance of the X-ray emission, internal free-free absorption of the radio emission, episodic or non-steady mass loss rate, asymmetry in the explosion seem to be common properties of this class of SNe.

Keywords radiation mechanisms: general; radiative transfer; stars: mass-loss; supernovae: general; X-rays: general; radio continuum: general

1 Introduction

A massive star (mass $M > 8M_{\odot}$) evolves for millions of years, burning nuclear fuel, and keeping the star stable with resulting outward radiation pressure. However, when the nuclear fuel in the star is exhausted, the equilibrium between gravity and radiation pressure ceases to exist and the star collapses under its own gravity within a fraction of a second. At some point the implosion turns into explosion, and a core-collapse supernova (SN) is born, leaving behind a relic which is either a neutron star or a black

¹ National Centre for Radio Astrophysics, Tata Institute of Fundamental Research, Pune University Campus, Ganeshkhind, Pune 411 007, INDIA

² Department of Astronomy, Stockholm University, AlbaNova, SE-106 91 Stockholm, SWEDEN
E-mail: poonam@ncra.tifr.res.in

hole. This is the most simplistic picture of a SN explosion. The classic paper by Brown and Bethe (1985) remains one of the best resources to get overall qualitative picture of the SN explosion. Understanding the detailed and quantitative characteristics of the explosion requires complex neutrino physics, general relativity and magneto-hydrodynamics. Other kind of supernovae (SNe), thermonuclear SNe, arising from the detonation of a white dwarf residing in a binary system are not the subject of this review.

Stars loose mass from their least gravitationally bound outermost layers. The mass loss rate \dot{M} from a massive star can be expressed as $\dot{M} = 4\pi r_\infty^2 \rho(r_\infty) v_\infty$, where $\rho(r_\infty)$ is the average mass density of the star at a distance r_∞ from the centre where the wind speed v_{wind} has reached terminal velocity v_∞ (Smith 2014). While Sun is losing mass at a rate of $\dot{M} \sim 10^{-14} M_\odot \text{ yr}^{-1}$, the massive stars loose mass more profusely owing to their much larger radii. The mass lost manifests itself in the form of dense winds moving with velocities of the order $10\text{--}1000 \text{ km s}^{-1}$, creating high density medium surrounding the star, a.k.a. circumstellar medium (CSM). The wind speed is generally proportional to the star's escape velocity, thus the outflows from the yellow super giants (YSGs) and red super giants (RSGs) with larger radii are normally slower ($\sim 10\text{--}20 \text{ km s}^{-1}$), whereas luminous blue variable (LBV) and blue super giants (BSGs) with smaller radii have faster winds ($\sim 100 \text{ km s}^{-1}$). In reality, though, high radiation from the SN can potentially accelerate the CSM winds to much higher speeds (Smith 2014).

In normal core-collapse SNe, the spectra and energetics are mainly governed by the explosion dynamics, and do not have imprints from the CSM. However, in a class of core-collapse SNe exploding in dense environments, termed as type II_n SNe (hereafter SNe II_n), the high CSM densities reveal their presence in the form of narrow emission lines in their optical spectra. While the radioactive decay mainly powers the optical light curves in normal core collapse SNe, the energetics has significant contribution from the SN explosion ejecta interacting with the dense CSM in SNe II_n, resulting in high bolometric and H- α luminosities (Chugai 1990). Due to this extra source of energy, they are detectable up to cosmological distances. The farthest detected Type II_n SN is at a redshift, $z = 2.36$ (Cooke et al 2009). SNe II_n are the focus of this review.

2 Progenitors of SNe II_n

The progenitor mass loss rates required to explain the extreme densities of SNe II_n are quite high, e.g. $10^{-3} - 10^{-1} M_\odot \text{ yr}^{-1}$. Chugai et al (2004) derived mass loss rate for SN 1994W to be $\sim 0.2 M_\odot \text{ yr}^{-1}$, whereas, the mass loss rate for SN 1995G was found to be $\sim 0.1 M_\odot \text{ yr}^{-1}$ (Chugai and Danziger 2003). In case of SN 1997ab, Salamanca et al (1998) argued that narrow P-Cygni profile superimposed on the broad emission lines implied a mass loss rate of $\sim 10^{-2} M_\odot \text{ yr}^{-1}$ for a presupernova wind velocity of 90 km s^{-1} . Chandra et al (2012a) and Chandra et al (2015) found mass loss rates $\sim 10^{-3} M_\odot \text{ yr}^{-1}$ and $\sim 10^{-1} M_\odot \text{ yr}^{-1}$ for SN 2006jd and SN 2010jl,

respectively. This indicates that the mass loss rates in SNe IIn are extremely high and not explained in standard stellar evolution theories of normal class of evolved stars, such as Wolf-Rayet (WR) star, LBVs, YSGs, RSGs etc (Fullerton et al 2006). One possibility is that such high mass loss rates may be related to an explosive event a few years before the SN outburst (Chugai and Danziger 2003, Pastorello et al 2007). Radiation production close to the Eddington limit can make the star unstable, which can lead to eruptive mass loss in a dramatically short time. However, the only stars which could incorporate enhanced mass loss shortly before explosion are super-asymptotic giant branch stars (AGB; mass $8 - 10 M_{\odot}$), massive RSGs (mass $17 - 25 M_{\odot}$) and LBV giant eruptions (mass $> 35 M_{\odot}$) (Fullerton et al 2006).

While erupting LBV progenitors are favorite models for bright SNe IIn because of their extreme mass loss rates (Humphreys et al 1999), they are a transient phase between O-type and WR stars (Humphreys and Davidson 1994), and are not supposed to explode at this phase. Even if they explode, the fine tuning of the explosion at the core coinciding with the enhanced episodic mass loss from the outer most layer is not understood. Yet archival data in some SNe IIn seem to suggest LBVs as progenitors, in particular SN 2005gl (Gal-Yam et al 2007), SN 2009ip (Mauerhan et al 2013), and SN 2010jl (Smith et al 2011). The pre-explosion Hubble Space Telescope (HST) suggested an LBV progenitor for SN 2005gl (Gal-Yam et al 2007). In addition, the inferred pre-shock wind speed of 420 km s^{-1} deduced from narrow hydrogen lines was also found to be consistent with the speeds of LBV eruptive winds (Smith et al 2010). In SN 2009ip, multiple pre-SN eruptions were observed before the star was finally thought to explode as SN IIn in 2012, strengthening the connection between SNe IIn and LBV progenitors (Mauerhan et al 2013). However, whether the 2012 event was a true SN is still debated (Fraser et al 2013). In case of SN 2010jl, pre-explosion archival HST data revealed a luminous, blue point source at the position of the SN, suggesting $M > 30 M_{\odot}$ LBV progenitor (Smith et al 2011). But recently Fox et al (2017) presented HST Wide-Field Camera (WFC3) imaging of the SN 2010jl field obtained 4 – 6 years after the SN explosion and showed that the SN is $0.61''$ offset from the blue source previously considered as the progenitor LBV star. The pre-SN eruptions have also been looked for and found in roughly half the SNe, in a sample of ~ 16 SNe IIn from the Palomar Transient Factory archival data (Ofek et al 2014a). However, these arguments were contradicted by Bilinski et al (2015), who analysed 12 years of Katzman Automatic Imaging Telescope archival data having five known SNe IIn locations and found no precursors. Anderson et al (2012) used H- α emission and near-ultraviolet (UV) emission as tracers of ongoing (< 16 Myr old) and recent ($16 - 100$ Myr old) star formation, respectively. He used pixel statistics to build distributions of associations of different types of SNe with host galaxy star formation. His sample of 19 SNe IIn was found to trace the recent star formation but not the ongoing star formation. Under the assumption that more massive stars have shorter life times, this implied that contrary to general belief majority of SNe IIn do not arise from the most massive stars. This was also suggested by Chugai

and Danziger (1994) based on the low ejecta mass $M_{\text{ej}} < 1M_{\odot}$ in SN 1988Z. In addition, Sanders et al (2013) reported the detection of another interactive kind (Type Ibn) of SN, PS1-12sk, in a giant elliptical galaxy CGCG 208-042 ($z = 0.054$), with no evidence for ongoing star formation at the explosion site. This further challenges the idea of interacting SNe arising from very massive progenitor stars, and puts a question mark on the LBV progenitors.

In addition, questions have been raised over the true nature of LBVs. Smith and Tombleson (2015) challenged the current understanding of LBVs, i.e. they being a transient phase between O-type and WR stars. They found that the LBVs are not spatially located in O-type clusters and are statistically more isolated than O-type and WR stars. Based on the relatively isolated environments of LBVs, they suggested that LBVs are product of binary evolution. They explained LBVs to be evolved massive blue stragglers. Smith et al (2016) took late time HST observations of the SN 2009ip site to search for evidence of recent star formation in the local environment, and found none within a few kpc. If LBVs are indeed transient phase between O-type and WR stars, they should be found in the massive star forming regions. They proposed that SN 2009ip progenitor may have been the product of a merger or binary mass transfer, rejuvenated after 4–5 Myr.

Even though LBVs remain the most favoured and exotic progenitors of SNe IIn, alternative models too have been suggested. Chugai and Danziger (1994), Chevalier (2012) proposed a binary model where common envelope evolution can give rise to SNe IIn. In this model, the SN is triggered by the inspiral of a compact neutron star or black hole to the central core of the binary star. Pulsational pair instability models too have been suggested, especially in Type IIn SLSNe, e.g. SN 2006gy (Woosley et al 2007). Quataert and Shiode (2012) proposed a gravity-wave driven mass loss model for such SNe IIn. According to this model, the fusion luminosity post C-burning stage can reach super-Eddington and generate gravity wave in massive stars. As the gravity waves propagate towards stellar surface, they can convert into sound waves and dissipation of the sound waves can trigger a sudden enhanced mass loss.

Overall, there is a large discrepancy in the progenitor models of SNe IIn. The heart of the problem is that SNe IIn classification is an external one, where any explosion surrounded by very high density can mimic a type IIn SN. Thus SNe IIn are governed by external factors rather than by internal explosion dynamics. Recently some superluminous supernovae (SLSNe) have also been explained in the extreme ejecta-CS interaction scenario by Chevalier and Irwin (2011). These are expected to be the extreme version of SNe IIn (Quimby et al 2013). Thus SNe IIn certainly encompass objects of different stellar evolution and mass loss history. For example, SN 1994W had a very fast decline after about > 125 days (Sollerman et al 1998), contrary to SN 1988Z which remained bright for a very long time (Turatto et al 1993). SN 1998S was initially classified as a bright Type IIL SN, however, at a very early stage (< 10 days) it started to show characteristics of type IIn SN (Li et al 1998). A special class of SNe IIn is characterized by spectral similarities to Type Ia SNe at peak light, but later shows SN IIn properties,

e.g., SNe 2002ic, 2005gj, PTF 11kx. While the explosion mechanism is not determined in the first two SNe, PTF 11kx was clearly considered to be a thermonuclear event (Dilday et al 2012). Some SNe IIn also appear to be related to Type Ib/c SNe. For example, SNe 2001em and 2014C were initially classified as type Ib SNe, however, at late epochs, signatures of the dense CSM interaction were found and these SNe were reclassified as SNe IIn (Chugai and Chevalier 2006, Milisavljevic et al 2015). These are not the unique SNe Ib/c to show late time CSM interaction signatures. While analysing a sample of 183 SNe Ib/c, Margutti et al (2017) found these late rebrightenings in SNe 2003gk, 2007bg, and PTF11qcj as well.

A well sampled long term observational follow up of ejecta-CSM interaction is the key to unravel the true nature of the SNe IIn progenitors through their footprints in their light curve and spectra.

3 Circumstellar Interaction

After a SN explosion, the shock wave propagates through the star and after shock breakout the expanding ejecta start to interact with the surrounding medium. While the inner part of the ejecta density profile is flatter, it is less important for the ejecta-CSM interaction dynamics. The outer ejecta density profile, more relevant part for the interaction, can be described as $\rho_{ej} = \rho_o(t/t_o)^{-3}(V_o t/r)^n$ (where for a mass element m_i , ejecta velocity $V(m_i)$, radius $r(m_i)$ and density $\rho(m_i)$ have time dependence of $r(m_i) = V(m_i)t$ and $\rho(m_i) = \rho_o(m_i)(t_o/t)^3$, Chevalier and Fransson 2016). The factor t^{-3} comes due to free expansion of the gas.

The shocked ejecta moving through layers of stars is radiation dominated mediated by photons. However, eventually the photons will diffuse out, leading to disappearance of the radiation dominated shock and acceleration of the outer gas. The velocity of the accelerated outer gas drops with radius because of the decreasing flux, hence the inner gas would catch up with the outer gas. Since the ejecta velocity is still supersonic, a viscous shock will be formed, which will commence the interaction with the surrounding medium.

Diffusion of the photons will happen when the optical depth is smaller than the ratio of speed of light, c to ejecta velocity V_{ej} , i.e. $\leq c/V_{ej}$ and the photon diffusion time scale becomes comparable to that of age of the SN (Chevalier and Fransson 2016). In normal core-collapse SNe, the diffusion happens at the progenitor radius, in form of shock breakout and a huge amount of energy ($10^{46} - 10^{48}$ ergs, Matzner and McKee 1999, Chevalier and Fransson 2016) is released, mainly in extreme ultraviolet (EUV) to soft X-rays. The shock breakout time scale is small (~ 1 hr), and is followed by the optical peak due to radioactivity. However, in some SNe IIn (especially superluminous SNe IIn), the density of the medium surrounding the exploding star is so high that optical depth $\tau_{wind} > c/V_{ej}$, and the shock breakout will happen in the CSM over a longer period of time, powering the bolometric light curve. Radiation from shock breakout can ionize and accelerate the immediate medium around it. Svirski et al (2012) have predicted generation of late time hard X-ray emission in these prolonged shock breakouts, which has been detected in a few SNe (Ofek et al 2013).

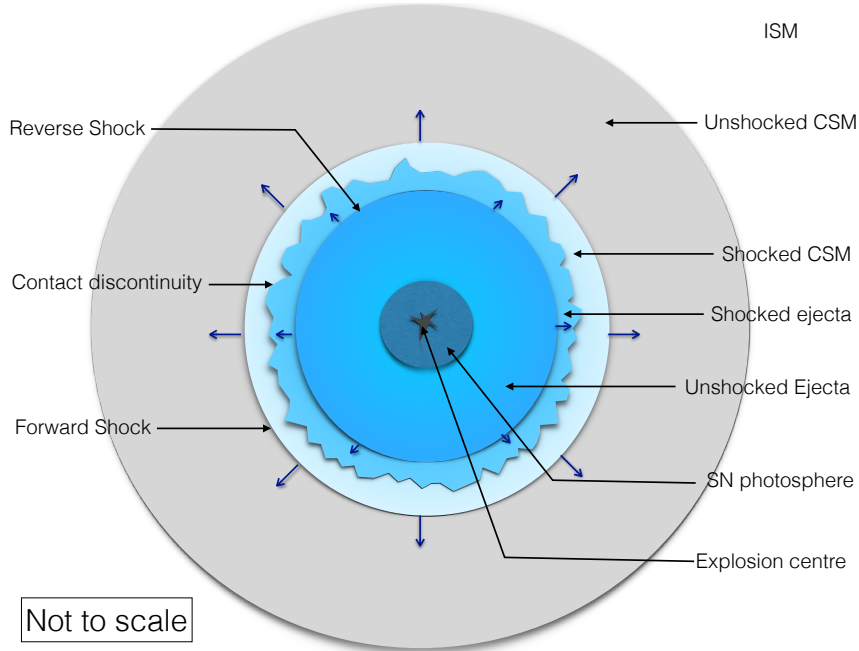


Fig. 1 Schematic diagram of a SN ejecta interacting with the surrounding CSM. This creates a hot 10^9 K forward shock, a 10^7 K reverse shock and a contact discontinuity in between. Hot forward and reverse shocks produce X-ray emission, whereas the electrons accelerated in the forward shock in the presence of the enhanced magnetic field produce synchrotron radio emission. Reprocessed X-ray can also come out as optical and UV radiation.

The structure of the unshocked CSM is important for the further ejecta-CSM interaction post shock-breakout. The CSM density profile ρ_{wind} depends upon mass loss rate as $\rho_{\text{wind}}(r) = \dot{M}/4\pi r^{-s} v_{\text{wind}}$ (where $s = 2$ for a steady wind). Thus if one has information of the ρ_{wind} , mass loss rate of the progenitor star can be estimated, provided the wind velocity is known. The fast moving ejecta collides with the CSM leading to the formation of a ‘forward’ shock moving in the CSM and a ‘reverse’ shock propagating back into the stellar envelope *relative to the expanding stellar ejecta* (Fig. 1 and Chevalier 1981, 1982a). In between the forward and the reverse shocks there exists a contact discontinuity, which is anything but smooth due to the instabilities in the region caused by low density shocked CSM decelerating high density shocked ejecta. The forward shock has a velocity of the order $10,000 \text{ km s}^{-1}$ and temperature $\sim 10^9$ K, whereas the reverse shock moves with velocity $\sim 1000 \text{ km s}^{-1}$, heating the stellar ejecta to $\sim 10^7$ K. The main consequences of the ejecta-CSM interaction is production of X-ray and radio emission (Chevalier 1982b, Chevalier and Fransson 2003, 2016). An analytical model of the emission due to ejecta-CSM interaction in SNe was developed by Chevalier (1982b), in which ejecta moves freely for several years in the ejecta dominated phase (mass of the ejecta is larger than the swept-up CSM mass). In normal core-collapse SNe, it takes several

thousands of years for the swept-up CSM mass to be significant enough (as compared to the ejecta mass) to slow down the free moving ejecta. However, in SNe IIn, the extremely dense CSM can substantially decelerate the SN ejecta very quickly, and converts ejecta kinetic energy into radiation very efficiently. This also causes the forward shock to cool radiatively and collapse into a cool dense shell.

Since the shock velocities are typically 100–1000 times the speed of the progenitor winds, the shock wave samples the wind lost many hundreds–thousands of years ago and thus probes the past history of the star.

When the interaction region between the forward and reverse shocks is treated in a thin-shell approximation, the shock front evolution is characterized by a self-similar solution (Chevalier 1981, 1982a,b). By balancing the ram pressure from the CSM and the ejecta, one can derive the the shock radii R_s expansion, which is a power law in time as $R_s \propto t^m$ ($m = (n-3)/(n-2)$). These solutions are valid for $n > 5$ to meet the finite energy constraints (Matzner and McKee 1999).

Chevalier and Fransson (2016) have given treatment to obtain various shock parameters. Please refer to it for details. Here I write down the main equations needed to interpret the observational data. Throughout the chapter, the subscript ‘CS’ refers to circumstellar shock and ‘rev’ to reverse shock.

The swept up masses behind the two shocks can be written as

$$M_{\text{CS}} = \frac{\dot{M} R_s}{v_{\text{wind}}} \quad (1)$$

$$M_{\text{rev}} = 4\pi \int_{R_s}^{\infty} \rho(r) r^2 dr$$

Since $\rho_{\text{rev}}/\rho_{\text{CS}} = \rho_{\text{ej}}/\rho_{\text{wind}}$, the masses and the densities of the shocked shells are related as

$$M_{\text{rev}} = \frac{(n-4)}{2} M_{\text{CS}} \quad (2)$$

$$\rho_{\text{rev}} = \frac{(n-4)(n-3)}{2} \rho_{\text{CS}}$$

The maximum ejecta velocity V_{ej} , circumstellar shock velocity at the contact discontinuity V_s , and reverse shock velocity V_{rev} can be written as

$$V_{\text{ej}} = R_s/t \propto t^{-1/(n-2)} \quad (3)$$

$$V_s = dR_s/dt = (n-3)/(n-2) V_{\text{ej}}$$

$$V_{\text{rev}} = V_{\text{ej}} - V_s = V_{\text{ej}}/(n-2)$$

Temperature of the forward CSM shock T_{CS} (assuming cosmic abundances), and that of the reverse shock T_{rev} are

$$kT_{\text{CS}} = 117 \left(\frac{n-3}{n-2} \right)^2 \left(\frac{V_{\text{ej}}}{10^4 \text{ km s}^{-1}} \right)^2 \text{ keV} \quad (4)$$

$$kT_{\text{rev}} = \frac{T_{\text{CSM}}}{(n-3)^2} = 1.2 \left(\frac{10}{n-2} \right)^2 \left(\frac{V_{\text{ej}}}{10^4 \text{ km s}^{-1}} \right)^2 \text{ keV}$$

The above equations assume the equipartition between ions and electrons, characteristic time to attain that is

$$t_{\text{eq}} = 2.5 \times 10^7 \left(\frac{T_e}{10^9 \text{ K}} \right)^{1.5} \left(\frac{n_e}{10^7 \text{ cm}^{-3}} \right)^{-1} \text{ s} \quad (5)$$

The ratio of the electron temperatures of the shocked CSM and shocked ejecta is $(n-3)^2$. While due to low temperature and higher density, the condition of equipartition between ions and electrons may be valid in the reverse shock, it is highly unlikely for the forward shock to obtain electron ion equilibrium. However, in SNe IIn, it is possible to meet this condition for both reverse as well as forward shocks owing to their extreme densities.

3.1 Radiation in ejecta CSM interaction

During ejecta CSM interaction in SNe, radiation can come in multiple frequency bands from the shocked as well as unshocked regions via multiple channels.

In the shocked CSM, the photospheric photons may undergo inverse-Compton (IC) scattering by the energetic electrons and may emit in UV and X-rays. For an electron scattering optical depth τ_e with $\tau_e < 1$ behind the CSM, a fraction τ_e^N electrons will scatter N times and boost their energies to UV and X-ray with a power-law spectrum of spectral index between -1 to -3 (Chevalier and Fransson 2003).

In addition, forward and reverse shocks are very hot (Eq. 5) and can emit soft and hard X-rays by free-free bremsstrahlung radiation. The total X-ray luminosity in free-free emission depends upon the medium density ρ_i (where subscript i refers to ‘CS’ and ‘rev’ for circumstellar and reverse shocks, respectively), and the emitting volume, which is proportional to R_s^3 . If Λ is the cooling function such that $\Lambda \sim T^{0.5}$ (Chevalier and Fransson 1994), then the X-ray luminosity can be written as $L_i \propto \rho_i^2 R_s^3 \Lambda$ (Fransson et al 1996). Chevalier and Fransson (2003) derives the expression for the free-free X-ray luminosity from the forward and reverse shocks to be

$$L_i \approx 3.0 \times 10^{39} \bar{g}_{\text{ff}} C_n \left(\frac{\dot{M}}{10^{-5} M_{\odot} \text{ yr}^{-1}} \right)^2 \left(\frac{v_{\text{wind}}}{10 \text{ km s}^{-1}} \right)^2 \left(\frac{t}{10 \text{ day}} \right)^{-1} \text{ ergs}^{-1} \quad (6)$$

Here C_n depends on the ejecta density index, and is 1 for the forward shock and $(n-3)(n-4)^2/4(n-2)$ for the reverse shock. The \bar{g}_{ff} is the free-free

Gaunt factor. A caveat to note here is that this equation is valid only under electron-ion equipartition which is questionable for the forward shock.

The Eq. 6 suggests that the free-free X-ray luminosity evolves as t^{-1} . However this is valid only for the constant density medium ($s = 2$). For a general case, Fransson et al (1996) derive the X-ray luminosity evolution to be

$$L_i \propto t^{-(12-7s+2ns-3n)/(n-s)}$$

An important point is that this formula assumes the X-ray emission covering the full X-ray band, whereas the X-ray satellites observe only in a very narrow band, e.g. *Chandra* and *XMM-Newton* cover 0.2–10 keV range. This means unless the luminosity ratio in the narrow observing band is same as that in the total X-ray band, one will not see the above evolution of the X-ray luminosity. As shown in Fransson et al (1996), the luminosity in a given energy band with $E < kT_i$ can be written as $L_i \propto t^{-(6-5s+2ns-3n)/(n-s)}$, which has a much flatter time dependence. For steady wind ($s = 2$) is, it will be $L_i \propto t^{-(n-4)/(n-2)}$.

The above treatment is valid for adiabatic shocks with $T > 2 \times 10^7$ K. For high mass loss rates and slow moving shocks, the radiative cooling may be important as cooling function will depend on temperature as $\Lambda \propto T^{-0.6}$ (Chevalier and Fransson 1994). If the temperature of the shocks goes below 2×10^7 K, then the efficient radiative cooling will lower the ejecta temperature to 10^4 K, where photoelectric heating from the shocks balances the cooling. Since the ram pressure is maintained, a cool dense shell (CDS) will form. The column density of the CDS can be estimated from $N_{\text{cool}} = M_{\text{rev}}/4\pi R_s^2 m_p$ (m_p is mass of a proton; Chevalier and Fransson 2003), which can be simplified to

$$N_{\text{cool}}(\text{RS}) \sim 10^{21}(n-4) \left(\frac{\dot{M}}{10^{-5} M_{\odot} \text{ yr}^{-1}} \right) \left(\frac{v_{\text{wind}}}{10 \text{ km s}^{-1}} \right) \left(\frac{V_{\text{ej}}}{10^4 \text{ km s}^{-1}} \right)^{-1} \left(\frac{t}{100 \text{ days}} \right)^{-1} \text{ cm}^{-2} \quad (7)$$

The effect of the CDS is that it will absorb the soft X-rays emission from the reverse shock and re-radiate into UV and optical emission and will contribute significantly to bolometric luminosity (Fransson 1984). In the CDS, the atoms recombine and produce mainly $\text{H}\alpha$ emission lines of intermediate line widths $\sim 1000 \text{ km s}^{-1}$.

Even though the intrinsic X-ray luminosity is high from the reverse shock owing to its high density, due to absorption of the emission (Nymark et al 2006), the X-ray emission may be dominated by the forward shock, especially in SNe IIn (Chandra et al 2012a, 2015). An additional factor favoring the dominance of the forward shock is that once the reverse shock becomes radiative, its luminosity rises proportional to density while the luminosity from the adiabatic forward shock continues to grow as density squared. If the mass loss rate is very high, even the forward shock may become radiative (e.g. SN 2010jl, Chandra et al 2015).

While the radiation due to ejecta-CSM interaction in SNe is affected by complicated hydrodynamics, in a simple approach the radiation luminosity of the shocks is the total kinetic luminosity times the radiation efficiency

$\eta = t/(t + t_c)$, where t_c is the cooling time of the shocked shell at the age t . In normal core-collapse SNe, the total radiated energy is only a few per cent of its kinetic energy, but could reach up to 50% in SNe IIn due to efficient cooling (Smith 2016). In case of the radiative forward and reverse shocks, the kinetic luminosity can be written as (Chevalier and Fransson 2016)

$$L_i = \pi R_s^2 (1/2 \rho_i V_i^3) = c_i \frac{(n-3)}{(n-2)} \times \frac{1}{2} \frac{\dot{M} V_{ej}^3}{v_{wind}} \quad (8)$$

Here $c_i = (n-4)/2(n-2)^2$ for the reverse shock and $c_i = (n-3)^2/(n-2)^2$ for the forward shock. Thus radiative luminosity goes as $L_i \propto t^{-3/(n-2)}$ for steady wind. However, for more general case, it will evolve as $L_i \propto t^{-(15-6s+ns-2n)/(n-s)}$.

While the X-ray emission discussed above are from the shocked shells, the unshocked ejecta and CSM can also contribute to significant radiation. During the shock breakout, the unshocked CSM can be ionized and emit in optical and UV bands by subsequent recombination, mainly in H α , Lyman- α and C III, C IV, N V, and Si IV, whose line widths gives information about the wind velocity. The unshocked CSM can also be excited by the X-rays from the forward and reverse shocked shells and can produce coronal emission lines, e.g., Fe VII and Fe X lines. The outermost layers of the unshocked ejecta, ionized and heated by radiation can contribute towards broad emission and absorption lines, such as C III, C IV, N V, and Si IV. In dense CSM, the electron scattering can be a dominant scattering and broaden the width of the above discussed emission lines.

The above treatment assumes spherical symmetry of the system. However, if the CSM is asymmetric and/or clumpy, there are strong observational consequences for the CSM interaction with the SN ejecta (Chugai and Danziger 1994). In a clumpy CSM, the predominance of soft radiation is likely to come out from the clumps, since due to high density the velocity of the shock in the clump will be much smaller than the $V_c = V_s(\rho_s/\rho_c)^{1/2}$. The higher density and lower velocity of the clump can lead to radiative cooling of the clump shock. Indeed, if the bulk of the CSM were in clumps, radiation from clumps become the dominant source of the radiation in the soft XUV band.

The ejecta diagnostics based on the CSM interaction cannot constrain the ejecta mass and energy uniquely because the same density versus velocity distribution in the ejecta outer layers can be produced by a different combination of mass and energy. Yet the observed interaction luminosity and the final velocity V_f of the decelerated shell constrain the energy of the outer ejecta from the condition $V > V_f$. For the power-law index n in $\rho_{ej} \propto r^{-n}$, the obvious relations, such as the ejecta density turnover velocity $V_0 \propto (E/M)^{1/2}$, $\rho(V) \propto \rho_0(V_0/V)^n$, and $\rho_0 \propto M/V^3$ result in the energy-mass scaling $E \propto M^{(n-5)/(n-3)}$. This scaling, when combined with the requirement that the velocity V_f should be larger than V_0 , provides us with the lowest plausible values of E and M .

An important consequence of ejecta-CSM interaction is the radio emission. In the fast moving forward shock, the particles can be accelerated

to relativistic energies, in the presence of magnetic field give rise to non-thermal synchrotron radio emission, which we discuss below.

3.1.1 Radio emission

In the shock front, the charged particles are accelerated most likely via diffusive Fermi shock acceleration (Blandford and Ostriker 1978, Bell 1978). The magnetic field is most likely the seed CSM magnetic field, compressed and enhanced in the shocked region. Rayleigh-Taylor instabilities at the contact discontinuity can further enhance the magnetic field (Chevalier and Blondin 1995). If the energy density of the magnetic field as well as the relativistic particles are considered to be proportional to the thermal energy density, then one can easily obtain the radio emission formulae.

Radio emission arises primarily from the higher temperature forward shock, where it is easier to accelerate the particles to relativistic energies. The electron energy distribution is assumed to be a power law $N(E) = N_o E^{-p}$, where E is the electron energy, N_o is the normalization of the distribution and p is the electron energy index, which is related to spectral index α (in $F_\nu \propto \nu^{-\alpha}$, where F_ν is the radio flux density at frequency ν) as $\alpha = (p - 1)/2$.

The radio emission is affected by either the external free-free absorption (FFA) process by the surrounding ionized wind, or by the internal synchrotron self absorption (SSA) by the same electrons responsible for the emission. The dominance of the absorption mechanism depends upon the mass loss rate, magnetic field in the shocked shells, shock velocity and density of the ejecta. One can distinguish between the two process from the optically thick part of the light curve or spectrum.

If SSA is the dominant absorption mechanism, then for SSA optical depth τ_ν^{SSA} , one can use Chevalier (1998) formulation to derive radio flux density evolution.

$$F_\nu^{\text{SSA}} = \frac{\pi R_s^2 c_5}{D^2 c_6} B^{-1/2} \left(\frac{\nu}{2c_1} \right)^{5/2} [1 - \exp(-\tau_\nu^{\text{SSA}})] \quad (9)$$

$$\tau_\nu^{\text{SSA}} = \int_0^s \kappa(\nu) ds \approx \kappa(\nu) s = \left(\frac{\nu}{2c_1} \right)^{-\frac{p+4}{2}} \left(\frac{4f R_s c_6 N_o B^{\frac{p+2}{2}}}{3} \right)$$

where c_1 , c_5 and c_6 are the constants defined in Pacholczyk (1970), D , and f , and B are the distance to the SN from observer, filling factor and magnetic field strength, respectively.

One can determine N_o from $\int_{E_l}^\infty N(E) E dE$, assuming electron rest mass energy to be the lower energy limit, i.e. $E_l = 0.51$ MeV, then

$$N_o = \frac{a B^2 (p - 2) E_l^{p-2}}{8\pi}$$

where a is the equipartition factor. The above equation can be written in terms of optically thick $\tau > 1$ and optically thin $\tau \leq 1$ limits as

$$F_{\nu}^{\text{SSA}}|_{\tau \leq 1} = \frac{4\pi f R^3}{3D^2} c_5 N_o B^{\frac{p+1}{2}} \left(\frac{\nu}{2c_1} \right)^{-\frac{p-1}{2}} \quad (10)$$

$$F_{\nu}^{\text{SSA}}|_{\tau > 1} = \frac{\pi R^2}{D^2} \frac{c_5}{c_6} B^{-1/2} \left(\frac{\nu}{2c_1} \right)^{5/2}$$

From these equations, one can estimate the R_p and B_p at the peak of the spectrum, when F_{ν}^{SSA} is F_p . They will depend on various parameters as

$$R_p \propto a^{-\frac{1}{2p+13}} f^{-\frac{1}{2p+13}} (p-2)^{-\frac{1}{2p+13}} F_p^{\frac{p+6}{2p+13}} D^{\frac{2p+12}{2p+13}} \nu^{-1} \quad (11)$$

$$B_p \propto a^{-\frac{4}{2p+13}} f^{-\frac{4}{2p+13}} (p-2)^{-\frac{4}{2p+13}} F_p^{-\frac{2}{2p+13}} D^{-\frac{4}{2p+13}} \nu$$

Chevalier (1998) has given these equations for $p = 3$ to be:

$$R_p = 8.8 \times 10^{15} a^{-\frac{1}{19}} \left(\frac{f}{0.5} \right)^{-\frac{1}{19}} \left(\frac{F_p}{\text{Jy}} \right)^{\frac{9}{19}} \left(\frac{D}{\text{Mpc}} \right)^{\frac{18}{19}} \left(\frac{\nu}{5 \text{ GHz}} \right)^{-1} \text{ cm} \quad (12)$$

$$B_p = 0.58 a^{-\frac{4}{19}} \left(\frac{f}{0.5} \right)^{-\frac{4}{19}} \left(\frac{F_p}{\text{Jy}} \right)^{-\frac{2}{19}} \left(\frac{D}{\text{Mpc}} \right)^{-\frac{4}{19}} \left(\frac{\nu}{5 \text{ GHz}} \right) G$$

In Eq. 12, if R can be measured in some independent way (e.g. VLBI), then both the magnetic field and the column density of the relativistic electrons can be determined. Another possibility to independently estimate the magnetic field is from synchrotron cooling effects, if it is observationally seen in the supernova spectrum. One can derive the exact equipartition fraction (e.g. SN 1993J, Chandra et al 2004).

By relating the post-shock magnetic energy density to the shock ram pressure, i.e. $B^2/8\pi = \varsigma \rho_{\text{wind}} V_s^2$, where ς ($\varsigma \leq 1$) is a numerical constant, mass loss rate to be obtained as

$$\dot{M} = \frac{6 \times 10^{-7}}{m_H^2 \varsigma} \left(\frac{B}{1 \text{ G}} \right)^2 \left(\frac{t}{100 \text{ d}} \right)^2 \left(\frac{v_{\text{wind}}}{10 \text{ km s}^{-1}} \right) M_{\odot} \text{ yr}^{-1} \quad (13)$$

While SSA seems to dominate in high velocity shocks, in the case of high mass loss rate, external free-free absorption may be quite dominant. Optical depth of the free-free absorption can be defined as

$$\tau_{\nu}^{\text{FFA}} = \int_{R_s}^{\infty} \kappa_{\nu}^{\text{FFA}} n_e n_i ds$$

Here $\kappa_{\nu}^{\text{FFA}}$ is the absorption coefficient, which depends upon n_e and n_i , the electron and ion number densities, respectively. Here $n_e = \dot{M}/4\pi R_s^2 v_{\text{wind}} \mu_e m_H$, and $n_i = \bar{Z} n_e$, where $\bar{Z} = \sum X_j Z_j^2 / \sum X_j Z_j$. Thus

$$\tau_{\nu}^{\text{FFA}} = \frac{\dot{M} \bar{Z} \kappa_{\nu}^{\text{FFA}}}{3(4\pi)^2 R_s^3 m_H^2 \mu_e^2 v_{\text{wind}}^2} \quad (14)$$

Panagia and Felli (1975), Weiler et al (2002) derived κ_ν^{FFA} to be

$$\kappa_\nu^{\text{FFA}} = 4.74 \times 10^{-27} \left(\frac{\nu}{1 \text{ GHz}} \right)^{-2.1} \left(\frac{T_e}{10^5 \text{ K}} \right)^{-1.35} \quad (15)$$

FFA will caused the radio emission arising out of the (mainly) forward shock to be attenuated by $\exp(-\tau_\nu^{\text{FFA}})$.

For fully ionized steady wind, and assuming the wind to be singly ionized, i.e. $\bar{Z} = 1$ and $\mu_e = 1.3$, will give mass loss rate to be

$$\dot{M} = 4.76 \times 10^{-5} (\tau_\nu^{\text{FFA}})^{0.5} \left(\frac{V_{\text{ej}}}{10^4 \text{ km s}^{-1}} \right)^{1.5} \left(\frac{t}{100 \text{ d}} \right)^{1.5} \left(\frac{T_e}{10^5 \text{ K}} \right)^{0.675} \left(\frac{v_{\text{wind}}}{10 \text{ km s}^{-1}} \right) \text{ M}_\odot \text{ yr}^{-1} \quad (16)$$

Here it is important to mention that the above formula will overestimate the mass loss rate if the wind is clumpy. Puls et al (2008) has shown that in clumpy wind, mass loss rate can change (to a lower value) by as much as a factor of 3.

In addition to SSA and FFA, Weiler et al (1990) proposed a model in which thermal absorbing gas is mixed into the synchrotron emitting gas. This can be a likely case with SNe IIn, in which a CDS is formed. A fraction of the cool gas ($10^4 - 10^5 \text{ K}$) from CDS mixed in the forward shocked region can also give rise to internal FFA. This will attenuate the radio emission by a factor $(1 - \exp(-\tau_\nu^{\text{intFFA}}))$, where τ_ν^{intFFA} is the internal FFA optical depth.

To fit the observational data, one can put above formulae in simpler forms, and derive time and frequency dependence of various parameters. When SSA is the dominant absorption mechanism, the data can be fit with the following model,

$$F_\nu(t) = K_1 \nu^{5/2} t^a (1 - \exp(-\tau_\nu^{\text{SSA}})) \quad (17)$$

$$\tau_\nu^{\text{SSA}} = K_2 \nu^{-(p+4)/2} t^{-(a+b)},$$

Here a gives the time evolution of the radio flux density in the optically thick phase ($F \propto t^a$) and b in the optically thin phase ($F \propto t^{-b}$). Under the assumption that the energy density in the particles and the fields is proportional to the postshock energy density, these quantities are related with expansion parameter m and electron energy index p as $a = 2m + 0.5$, and $b = (p + 5 - 6m)/2$.

When FFA is the dominant absorption mechanism, the evolution of the radio flux density can be fit with

$$F_\nu(t) = K_1 \nu^{-\alpha} t^{-\beta} \exp(-\tau_\nu^{\text{FFA}}(t)) \quad (18)$$

$$\tau_\nu^{\text{FFA}}(t) = K_2 \nu^{-2.1} t^{-\delta},$$

where α is the frequency spectral index, which relates to the electron energy index as $p = 2\alpha + 1$. Here K_1 is the radio flux density normalization

parameter and K_2 is the FFA optical depth normalization parameter. The parameter δ is related to the expansion parameter m in $R_s \propto t^m$ as $\delta \approx 3m$. The parameter β is the time dependence, which under the assumption that the energy density in the particles and the fields is proportional to the postshock energy density leads to $\beta = (p + 5 - 6m)/2$ (Chevalier 1982a,b).

When mixing of cool gas in the synchrotron emitting region is responsible for much of the absorption, in such a case the flux takes the form

$$F_\nu(t) = K_1 \nu^\alpha t^\beta \frac{(1 - \exp(-\tau_\nu^{\text{intFFA}}))}{\tau_\nu^{\text{intFFA}}} \quad (19)$$

$$\tau_\nu^{\text{intFFA}} = K_2 \nu^{-2.1} t^{\delta'},$$

where δ' is time evolution of internal-FFA optical depth.

Above discussion is based on the spherical geometry of the SN-CSM system. However, there is evidence that the ejecta and the CSM may be far from spherical and very complex in some cases. Smith et al (2009) found an anisotropic and clumpy CSM medium in the RSG VY CMa, whereas the structure of η Carinae was found to be bipolar (Smith 2010). The deviation from spherical geometry can have strong observational consequences in studying the SN-CSM interaction.

From this section onwards, I will concentrate on the observational aspects of SNe IIn, mainly in X-ray and radio bands.

4 X-ray observations of SNe IIn

Since high CSM density is a prerequisite for the radio and X-ray emission, the ejecta CSM interaction is expected to emit copiously in these bands in SNe IIn. However, the statistics is contradictory. While more than ~ 400 SNe IIn are known, only 12 are known to emit in the X-ray bands (Fig. 2). These include SNe 1978K, 1986J, 1988Z, 1995N, 1994W, 1996cr, 1998S, 2005ip, 2005kd, 2006gy, 2006jd and 2010jl (Ross and Dwarkadas 2017). In Fig. 2, we plot X-ray luminosities of SNe IIn in 0.3–8 keV and 0.5–2 keV bands. In 0.3–8 keV band, SNe IIn have high luminosities spread within an order of magnitude, with the exception of SNe 1978K and 1998S which are weaker X-ray emitters. Other than SN 2010jl, most of the X-ray detected SNe IIn have X-ray emission after around a year. This could have contribution from observational biases due to lack of early observations. However, recently, in SN 2017gas, a nearby ($d = 43$ Mpc) SN IIn, early observations covering 20–60 after the discovery resulted in a non-detection (Chandra and Chevalier 2017). In lower panel of Fig. 2, we plot X-ray luminosity of SNe IIn in soft X-ray band (0.5–2 keV). SN 2006gy is a weak X-ray emitter emitting only in the soft X-ray band. However, it was a SLSN and SLSNe are generally known to be weak X-ray emitters. Here the most unique SN is SN 1996cr, which was detected after 1000 days and since then it's luminosity continued to rise.

Due to higher density of the reverse shock, the thermal X-ray emission from core collapse SNe, in general, has dominating contribution from the

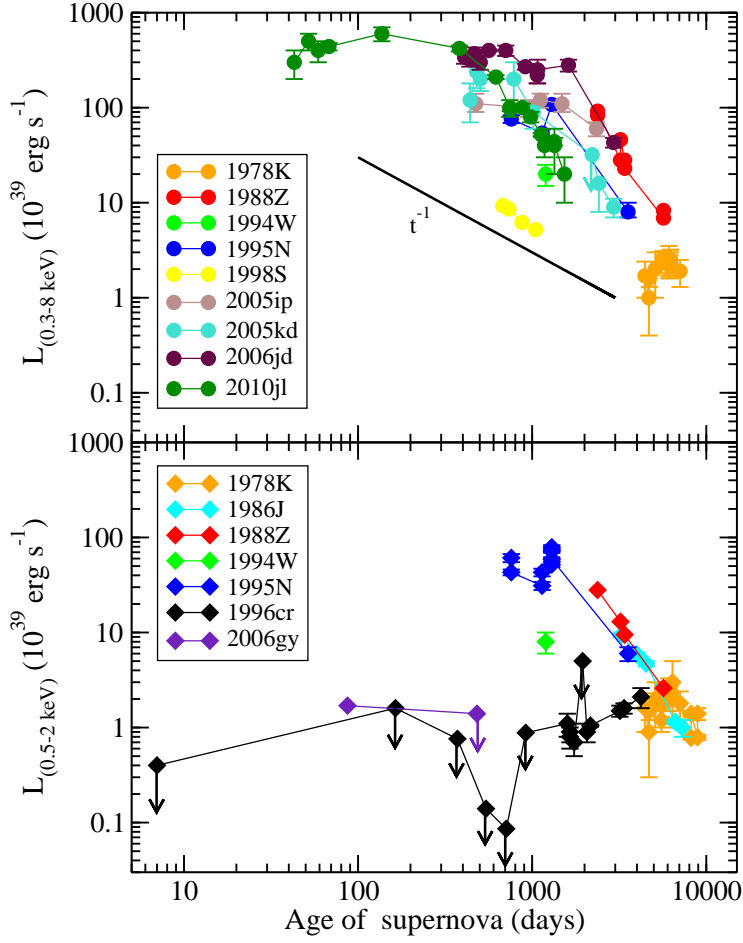


Fig. 2 The 0.3–8 keV (upper panel) and 0.5–2 keV (lower panel) X-ray luminosities of SNe IIn (Ross and Dwarkadas 2017). In the upper panel the X-ray luminosities of SN 1998S and SN 2006jd are in 0.2–10 keV and in the lower panel, SN 1986J and SN 1995N X-ray luminosities are in the range 0.5–2.4 keV.

reverse shock. In SNe IIn, the X-ray plasma temperatures have been found to be generally higher, consistent with the emission from the forward shock. In SN 2005ip, the X-rays were fit by temperature $T \geq 7$ keV, for at least upto 6 years after the explosion (Katsuda et al 2014). In SN 2005kd, the early emission (up to ≤ 2 years) was dominated by hard X-rays (Dwarkadas et al 2016). Chandra et al (2012a) have shown that the *Chandra* and *XMM-*

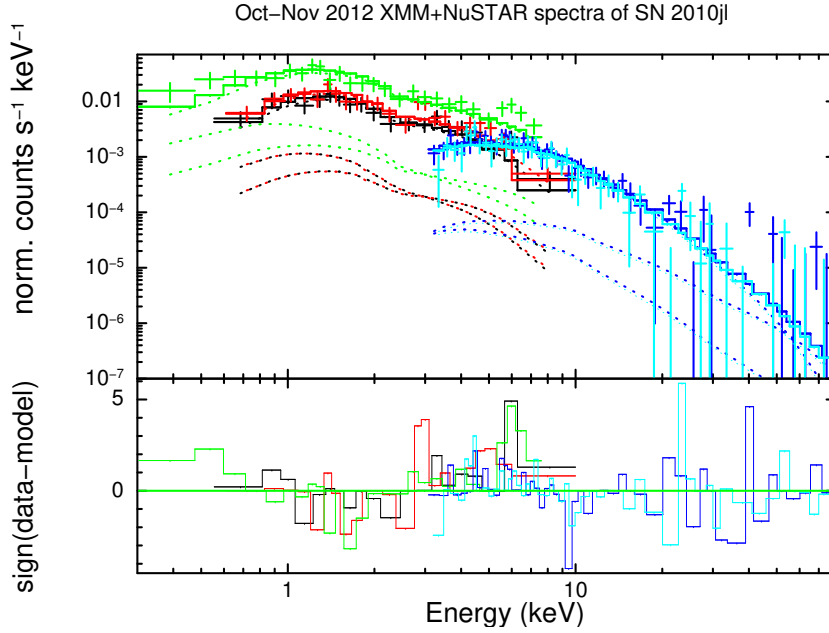


Fig. 3 Joint *NuSTAR* and *XMM-Newton* spectrum of the SN 2010jl covering energy range 0.3–80 keV. Chandra et al (reproduced from, 2015).

Newton observations in SN 2006jd are best fit with a thermal plasma with electron temperature ≥ 20 keV. This is because the radiative cooling shell (CDS) formed between the reverse and forward shock may have absorbed most of the X-rays emanating from the reverse shock. While this implies X-ray emission is mainly coming from the forward shock, these telescopes did not have the sensitivity to better constrain the temperature since both work below 10 keV range. In SN 2010jl, using the joint *NuSTAR* and *XMM-Newton* observations, Ofek et al (2014b), Chandra et al (2015) derived the X-ray spectrum in the energy range 0.3–80 keV, and constrained the X-ray emitting shock temperature to be 19 keV, thus confirming that the dominant X-ray emission in the SN is indeed coming from the hotter forward shock (Fig. 3). This is the first time the (forward) shock temperature was observationally accurately measured in a SNe IIn.

As discussed in section, §3, the thermal X-ray luminosity is expected to decline as $\sim 1/t$ for a steady wind. However, observations of several SNe IIn have shown to not follow this evolution (See Fig. 2 as well as Dwarkadas and Gruszko (2012), Dwarkadas et al (2016)). In the energy range 0.2 – 10 keV, where the current telescopes *Chandra*, *XMM-Newton* and *Swift-XRT* are most sensitive, SN 2005kd followed a X-ray luminosity evolution of $L_{\text{Xray}} \propto t^{-1.6}$ (Dwarkadas et al 2016). Contrary to it, SN 2006jd followed a flatter decline of $t^{-0.2}$ for upto 4.5 years (Chandra et al 2012a), followed by a much steeper decline 8 years later (Katsuda et al 2016). The X-ray luminosity for SN 2010jl was found to be roughly constant for the first

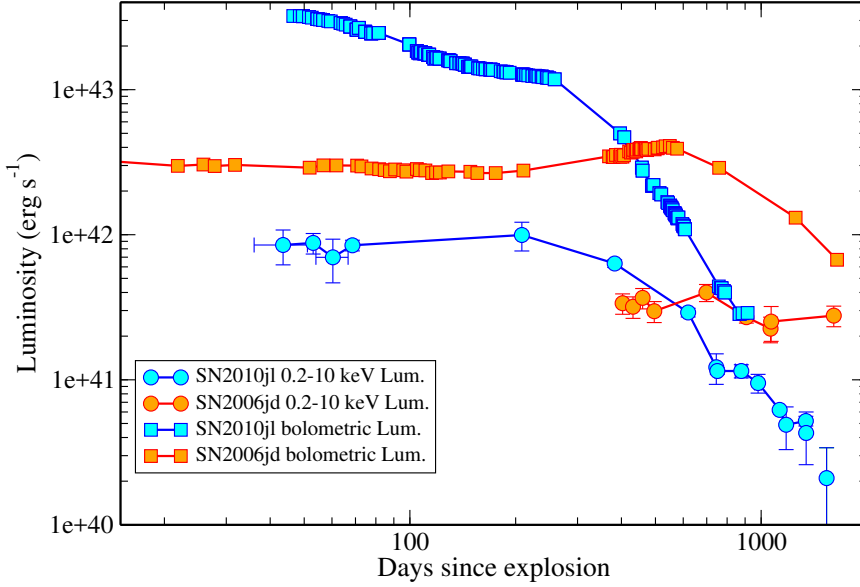


Fig. 4 The X-ray (filled circles) and bolometric luminosity (filled squares) evolution of SN 2006jd and SN 2010jl. The blue curves are for SN 2010jl and orange curves indicate SN 2006jd. None of them follow $\sim 1/t$ dependence. Chandra et al (reproduced from, 2015).

~ 200 days with a power-law index of $t^{0.13 \pm 0.08}$, followed by a much faster decay with a power-law index of $\sim -2.12 \pm 0.13$ after day 400. Unfortunately there are no data between 200 and 400 days to see the luminosity evolution in this range. Figure 4 shows the plot of X-ray and bolometric luminosity light curves of SN 2010jl and SN 2006jd. The deviation from t^{-1} is quite evident here. The luminosity decline is much flatter in SN 2006jd than that of SN 2010jl. Around the same epoch, the SN 2006jd X-ray light curve declines as $t^{-0.24}$, while SN 2010jl declines as $t^{-2.12}$. The relative flatness of the bolometric luminosity of SN 2006jd for a longer duration indicates that the CSM interaction powered the light curve for a much longer time than SN 2010jl. This indicates that the duration of mass ejection in SN 2006jd may have been longer in this case than for SN 2010jl, though in both cases it occurred shortly before the explosion. This suggests a different nature of progenitors for the two SNe.

While this deviation from $L_{\text{Xray}} \propto 1/t$ could be attributed to effects like inverse-Compton scattering etc. at early times, the late time deviation seen in many SNe IIn cannot be explained by it. The complex nature of the progenitor star of SNe IIn could also be a cause of this. If the winds are not steady (deviation from $\rho_{\text{wind}} \propto 1/R^2$), and has clumpy, asymmetric structure, the luminosity evolution will be far from $L_{\text{Xray}} \propto 1/t$. However, narrow energy ranges of present X-ray instruments pose a problem because of which one measures spectral X-ray luminosity, whereas the $\sim 1/t$ dependence is valid for total X-ray luminosity (Fransson et al 1996). As discussed

above, the observations have indicated that the temperatures of the X-ray emitting region in many SNe IIn are higher than can be measured in the 0.2–10 keV bandpass of the X-ray detectors, thus we may be missing the peak of the X-ray emission. A measurable effect of this instrument bias is that, as shock sweeps up more and more material with time, shock temperature decreases, shifting the X-ray emission to progressively lower temperatures at later epochs. Thus one should see flattening or even increase in the soft X-ray emission flux with time. This was seen in SN 1978K, where 2–10 keV flux showed decline, but 0.5–2 keV soft X-ray emission remained constant for a long time without any signs of decline (Schlegel et al 2004). However, there are exceptions like SN 1986J and SN 1988Z where soft X-ray luminosity was found to evolve as $L_{\text{Xray}} \propto t^{-3}$ (Temple et al 2005) and $L_{\text{Xray}} \propto t^{-2.6}$ (Schlegel and Petre 2006), respectively. This may suggest that more physical reasons (like complex progenitor, unsteady mass loss rates etc.) are responsible for this behaviour, other than the narrow bandpass of X-ray instruments. In this respect, SN 1996cr was a unique SN which demonstrated a factor of > 30 increase in X-ray flux between 1997 and 2000 (Bauer et al 2008). The observations implied that the progenitor of SN 1996cr exploded in a cavity and freely expanded for 1–2 before striking the dense CSM. The above observational study shows that it is crucial to have a wide band X-ray coverage to disentangle the instrumental issues from the physical reasons in order to truly understand the nature of the X-ray emission.

4.1 Evolution of column density

In some SNe IIn with well sampled X-ray observations, the X-ray column densities have seemed to evolve with time, indicating the cause of absorption as CSM contrary to ISM. Katsuda et al (2014) found column density of $N_H \sim 5 \times 10^{22} \text{ cm}^{-2}$ for first few years in SN 2005ip, gradually decreasing to $N_H \sim 4 \times 10^{20} \text{ cm}^{-2}$ at later epochs, consistent with the Galactic absorption. The fact that the spectra was fit well with a thermal emission model with $kT > 7 \text{ keV}$ implied forward shock origin of the X-rays absorbed by the evolving CSM.

SN 2010jl is the best studied Type IIn SN in X-ray bands, where X-ray observations covered a period up to day 1500 with *Chandra*, *XMM-Newton*, *NuSTAR*, and *Swift*-XRT. This SN provided the best studied evolution of column density from 40 to 1500 days (Fig. 5 and Chandra et al 2012b, 2015). During this time period, three orders of magnitude change in column density was witnessed. At first epoch the column density associated with the SN was $N_H = 10^{24} \text{ cm}^{-2}$, 3000 times higher than the Galactic column density, which declined slowly by an order of magnitude upto day ~ 650 . Followed by a sharp decline, it settled to 10 times the Galactic value. The higher column density observed in the X-ray observations for SN 2010jl was not found to be associated with the high host galaxy extinction, indicating that the higher column density is due to the mass loss near the forward shock and thus is arising from the CSM. This was the first time that external circumstellar

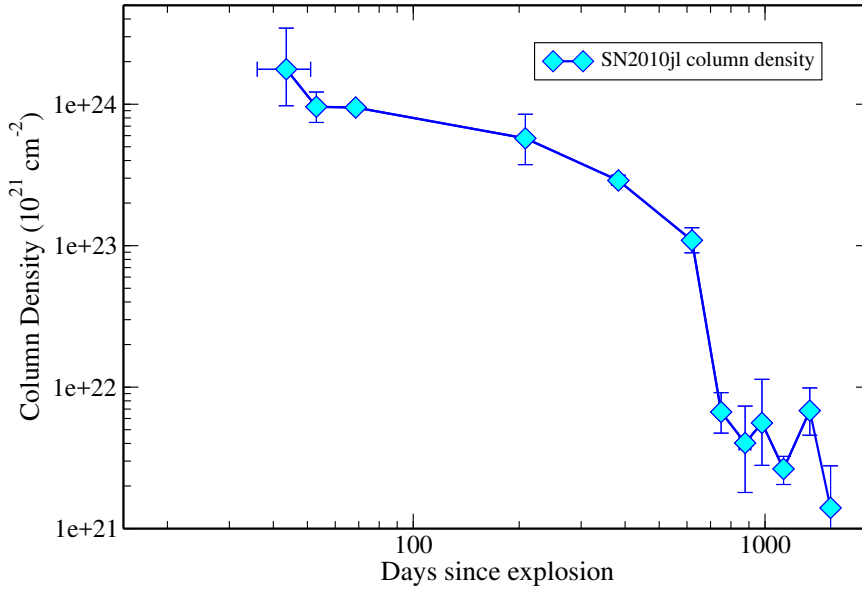


Fig. 5 The column density evolution in SN 2010jl. The figure is reproduced from Chandra et al (2015).

X-ray absorption had been clearly observed in a SN and enabled one to trace the precise mass loss evolution history of the star.

As discussed in previous section, due to high density of the CSM, much of the X-ray is reprocessed to visible bands. Thus one would expect less efficient reprocessing as material becomes more transparent with time. In the X-ray and bolometric luminosities plot of SN 2006jd and SN 2010jl (Fig. 4), the bolometric luminosities are at least an order of magnitude higher for first several hundred days. However, the difference between the two luminosities is decreasing with time. This indicates that with decreasing density, reprocessing of X-rays are becoming less efficient. Long term follow up of the X-ray and bolometric luminosities will be very informative here.

5 Radio emission of SNe IIn

Radio emission in SNe IIn is very intriguing. Out of ~ 400 , less than half SNe IIn (~ 154) have been looked in the radio bands (mainly with the Very Large Array (VLA)) and $\sim 10\%$ have been detected. However, there is a very interesting trend in radio and X-ray detected SNe IIn. While X-ray luminosities are towards the high end in SNe IIn, the radio luminosities are diverse. In Fig. 6, we plot peak X-ray and radio luminosities of radio and X-ray detected SNe IIn and compare them with some well sampled core collapse SNe. While the X-ray luminosities of SNe IIn are systematically higher than their counterparts, radio luminosities do not stand out and occupy four orders of magnitude space.

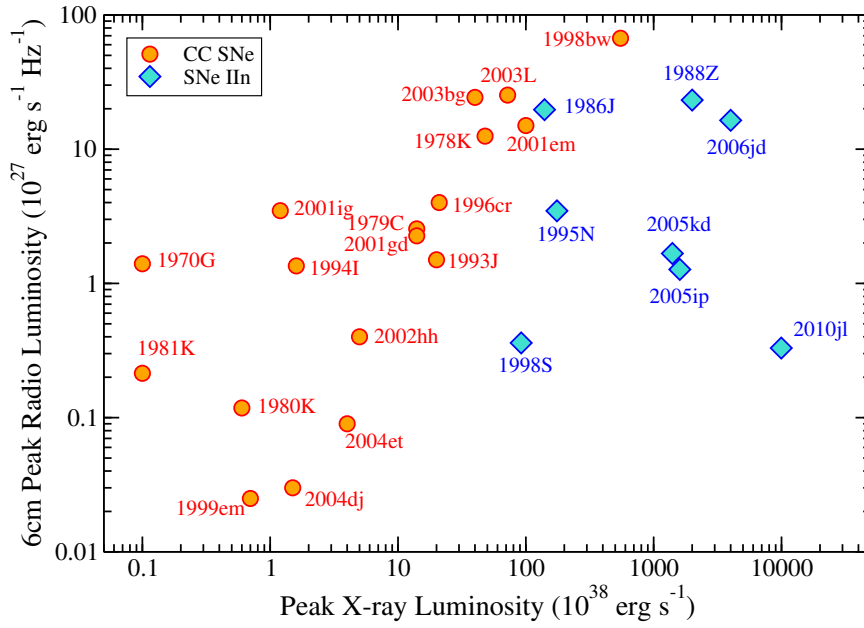


Fig. 6 Radio and X-ray peak luminosities of SNe IIn compared with some well observed core collapse SNe. While in radio bands SNe IIn do not stand out, they occupy higher values in the X-ray luminosity space. The X-ray data is taken from Immler (2007) and radio data mainly from Weiler et al (2002).

This probably could be explained as a side effect of high density. While high density of the CSM means efficient production of synchrotron radio emission, it also translates into higher absorption. Hence, by the time emission reaches optical depth of unity, the strength of synchrotron emission is already weakened. This can explain that radio light curves are extremely diverse; the diversity translate to diversity in the CSM density and could indicate the different mass loss history.

The support to above argument also comes from the fact that most of the SNe IIn are late radio emitters (Fig. 7), indicating higher absorption early on (Chandra et al., to be submitted). Some of the radio emitting SNe IIn were either discovered late or classified late. The prototypical SNe IIn, e.g. SN 1986J, SN 1988Z and SN 1978K were observed years after their explosions. Most of the SNe IIn discovered soon after the explosion, did not have early radio observations within a month, except for SN 2009ip (Margutti et al 2014). SN 2009ip was detected in radio bands early on but faded below detection within a few tens of days. However, SN 2009ip was a peculiar SN with poorly understood explosion mechanism. In contrast, the observations of SN 2010jl started by day 45 but the first detection happened only after 500 days (Chandra et al 2015), clearly showcasing the efficient absorption of radio emission for a long period.

In addition to high absorption, observational biases could also be partially responsible. The late radio turn on may also explain the observed

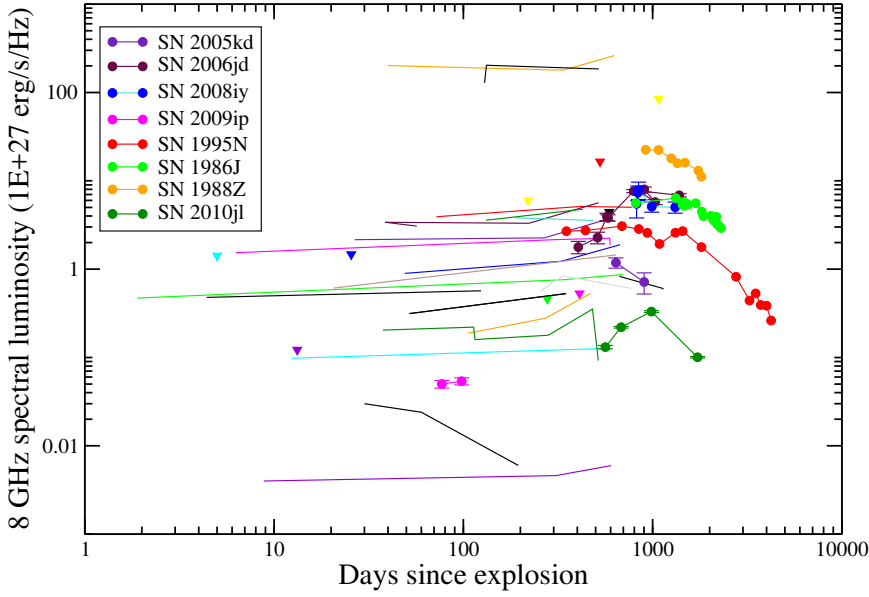


Fig. 7 8 GHz radio spectral luminosity of some of the well observed SNe II (Chandra et al. to be submitted). Here circles are detections. The lines indicate upper limits at observations at many epochs. Single triangles indicate upper limits at individual epoch.

overall low detection rates of SNe II. If a SN is not bright in radio bands in a first few epochs, the observational campaign for that SN is usually over. So even if a SN II was a potential radio emitter at later epochs, it would be missed in radio bands. To understand this observational bias, van Dyk et al (1996) observed 10 SNe II at an age of a few hundred days and still did not detect any; they set upper limits of $150 - 250 \mu\text{Jy}$. However, the current telescopes are able to reach at least an order of magnitude better sensitivity. In addition, the current upgraded VLA is extremely sensitive at higher frequencies where the radio absorption effects vanish much sooner ($\tau_\nu \propto \nu^{-2}$). Strategic study of SNe II at higher frequencies at early times to low frequencies at late epochs is likely to result in the most complete sample of radio supernovae (Perez-Torres et al 2015, Wang et al 2015).

5.1 Absorption of radio emission

In classic core collapse SNe, the radio emission is mainly absorbed either by the ionized CS medium (FFA) or by the in situ relativistic electrons (SSA). Observations when the SN is rising in the light curve evolution can disentangle the underlying absorption mechanism. The role of absorption mechanisms is different for different SNe (Chevalier and Fransson 2003). SNe II are expected to have external FFA due to their high density. However, in SNe II due to high density, radiative cooling shell is formed in the shocked region. The mixing of the cool gas in the forward shocked shell

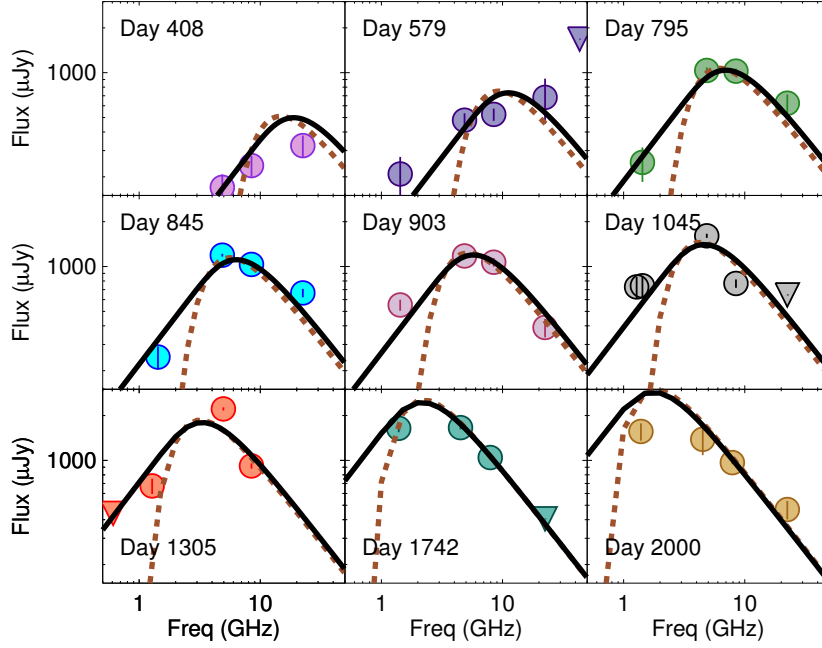


Fig. 8 Spectra of SN 2006jd reproduced from Chandra et al (2012a). Here internal free-free absorption (black solid lines) best fit the observed absorption.

may cause some SNe IIn to undergo internal FFA. This indeed has been seen in SN 2006jd (Fig. 8 and Chandra et al 2012a), SN 1986J (Chandra et al 2012a) and SN 1988Z (van Dyk et al 1993, Williams et al 2002).

In SN 2006jd, Chandra et al (2012a) estimated the mass of the mixed absorbing gas by assuming that the absorbing low temperature ($10^4 - 10^5$ K) gas is in pressure equilibrium with the X-ray emitting gas. They showed that modest amount of $\sim 10^4$ K cool gas, i.e. Mass $\sim 10^{-8} M_{\odot}$ could explain internal absorption in SN 2006jd (Fig. 8).

Irrespective of the fact whether absorption is internal or external, it implies very high mass loss rates. However, the mass loss rate constraints will become less severe by a factor of 3 if the wind is clumpy (Puls et al 2008). In addition, calculations of mass loss rate are usually done assuming solar metallicity. However, metallicity will lower mass loss rate as $\dot{M} \sim Z^{0.69}$ (Vink et al 2001). Interestingly, recent observational findings demonstrated that erratic mass-loss behavior preceding core-collapse extends to H-poor progenitors as well.

6 Episodic mass loss?

Multiwavelength observations of SNe IIn have shown that the mass loss rate from some SNe IIn may not be steady. Unfortunately it is difficult to dis-

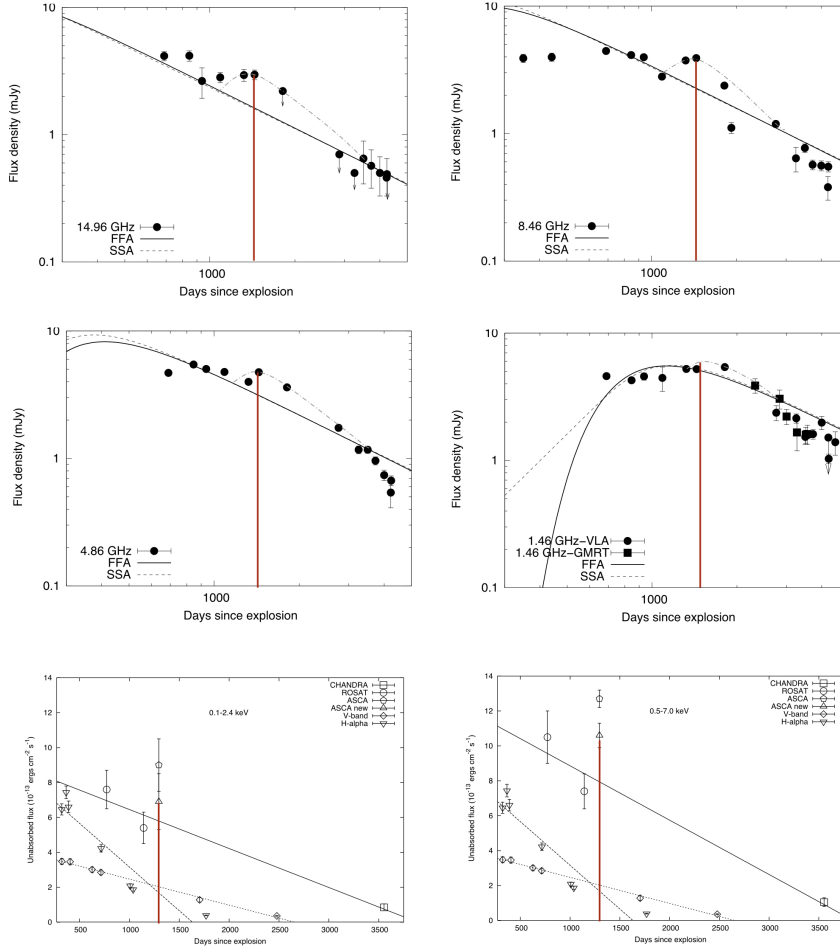


Fig. 9 Radio and X-ray light curves of SN 1995N. A hint of enhanced emission bump in radio and X-ray bands of a Type IIn SN 1995N around ~ 1300 days. The figure is reproduced from Chandra et al (2005, 2009).

entangle this effect because SNe IIn likely to remain highly absorbed for a long duration. By the time they become optically thin in radio bands, the strength of synchrotron emission is rather weak to see any modulations due to changing mass loss. In addition, one needs a long term follow up to see the episodic mass loss. In X-ray observations, due to the lack of well sampled data, such trends are easy to miss. Yet, it seems that some SNe IIn seem to suggest episodic mass loss rate.

In Fig. 9, X-ray and radio light curves are plotted for a Type IIn SN 1995N (Chandra et al 2009). The X-ray bands were chosen to mimic the *ROSAT* and *ASCA* bands (Chandra et al 2005). The radio data is at the four representative VLA frequencies. Around day ~ 1300 onwards, bumps

in the X-ray and radio light curves are seen. The long gap in the X-ray light curve does not allow us to witness the evolution of this bump, however, in the radio data one can clearly see this effect. Due to the sensitivity limitation of the telescopes and lack of long term follow up, its not possible to explore the further bumps, if any.

Hints of bumps near simultaneously in both X-ray and radio bands light curves can be possibly seen in SN 2006jd as well (Chandra et al 2012a). The radio emission is too weak in SN 2010jl to note any such bumps. However, X-ray data seems to suggest a steady decline followed by a sudden decline settling down to steady decline again at ~ 1000 days (Chandra et al 2015). These trends could be suggestive of the episodic mass loss rates in some SNe IIn and may support the LBV scenario. However, further study and much longer follow ups are needed. Episodic mass-loss rates have been seen in many type Ib/Ic/I Ib SNe too.

7 Asymmetry in the explosion

Although in normal core collapse SNe, circumstellar interaction can be successfully described in terms of spherical models, there are indications of more complex situation in SNe exploding in dense environments. In optical bands, there have been various pieces of evidence suggesting asymmetry in the explosion via polarization observations. The optical spectropolarimetry observations with Keck telescope showed a high degree of linear polarization in SN 1998S, implying significant asphericity for its CSM environment (Leonard et al 2000). In SN 1997eg, spectropolarimetric observations indicated the presence of a flattened disk-like CSM surrounding a aspherical ejecta, which Hoffman et al (2008) interpreted supporting the LBV progenitor scenario. Patat et al (2011) found significant polarization in SN 2010jl two weeks after the discovery, suggesting similarity with SN 1998S and SN 1997eg. Many of the models explaining SNe IIn require bipolar wind or disk like geometry (see Smith (2016) for a review).

In some SNe IIn, interpretation of the radio and X-ray data too seem to suggest asymmetry. In case of SN 2006jd, it was difficult to reconcile the X-ray and radio data with spherical models (Chandra et al 2012a). The column density of the matter absorbing the X-ray emission was found to be ~ 50 times smaller than what was needed to produce the X-ray luminosity. In addition, the implied column density from radio observations were also found to be low. Chandra et al (2012a) attempted to explain it with the clumpiness of the CSM clouds, since the absorption column depends on the CSM wind density as $\propto \rho_{\text{wind}}$ and the X-ray luminosity as $\propto \rho_{\text{wind}}^2$. However, it lead to inconsistent shock velocity derived from the observed X-ray spectrum and this model was ruled out. They explained it in a scenario in which the CSM clouds interact primarily with the CDS. This suggested that there is a global asymmetry in the CSM gas distribution that allowed a low column density in one direction, unaffected by the dense interaction taking place over much of the rest of the solid angle as viewed from the SN. This would also explain low column density to the radio emission too,

because both radio and X-ray are from the same region. The lack of external FFA seen in this SN could also be explained in this model.

SN 2010jl early optical spectra showed the presence of broad emission lines (Smith et al 2012, Fransson et al 2014, Ofek et al 2014b). This could be explained by an electron scattering optical depth $> 1 - 3$, i.e., a column density $N_H \geq 3 \times 10^{24} \text{ cm}^{-2}$. This was comparable with the column density seen in the first X-ray observations (Chandra et al 2012b). However, at later epochs ($t > 70$ day), X-rays column density declined to $N_H < 3 \times 10^{24} \text{ cm}^{-2}$. These constraints are difficult to reconcile with a spherical model of column density $3 \times 10^{24} \text{ cm}^{-2}$. This may suggest that the X-rays escape the interaction region, avoiding the high column density CSM. This situation can be reconciled well in a scenario for the CSM having a bipolar geometry.

If LBVs indeed are the progenitor of some SNe IIn, they are most likely asymmetric as known Galactic LBVs show a complex CSM structure. In addition, binary evolution can also lead to aspherical structure (e.g., McCray and Fransson 2016).

8 Summary and open problems

In this review, I have discussed the observational aspects of the ejecta-CSM interaction mainly in SNe exploding in dense environments. The review mainly concentrates on the radio and X-ray emission, with the aim of understanding the nature of intriguing progenitor system of SNe IIn.

Observations have indicated that in SNe IIn show high X-ray luminosities dominated by high temperatures for years, implying forward shock is responsible for the dominant X-ray emission. Long terms observations of X-ray emission have indicated evolving CSM in some SNe IIn, directly confirming the evidence that medium surrounding stars is modified via progenitor star, the properties of which can be studied by the detailed X-ray light curves and spectra. However, one need to make observations in wide X-ray bands, to avoid biases coming from the narrow X-ray range, thus to disentangle the observational effects versus the ones coming due to the nature of progenitor wind.

In radio bands, SNe IIn are mostly late emitters. Radio detected SNe IIn do not tend to be necessarily bright, most likely due to absorption. The absorption mechanism could have dominant contribution from the cool gas mixed in the radio emitting region. This could also be the reason that only 10% SNe IIn show radio emission. More systematic studies are needed to remove observational biases and pin point the physical causes of the low detection statistics. The property of late time turn on may be causing us to miss many of them due to lack of late enough observations. With the wealth of new and refurbished sensitive telescopes, a carefully planned sensitive study is needed. A good strategy is to observe SNe IIn at high frequencies for at least a year before discarding it as a radio non-emitter.

The nature of progenitor of SNe IIn remains the biggest challenge. The mass loss rates needed to explain SNe IIn are extremely high. Some SNe IIn have indicated episodic mass loss rates. There are hints of eruption events towards end stages of evolution. These effects need to be included in the

current generations of stellar evolution models. However, it is important to note here that the mass loss rate constraints will become less severe by a factor of 3 if the wind is clumpy.

Many of the massive stars are expected to live in binary systems. Their influence in the stellar evolution need to be explored. In addition, observations have indicated low progenitor masses in some SNe IIn. This has challenged the idea of interacting SNe arising from very massive progenitor stars, and has put a question mark on the LBV progenitors. In fact, the very nature of the LBV has been questioned and much work is needed in this direction. A very sensitive observations of the Galactic OB regions and LBV stars could throw light on this.

Acknowledgements I thank referee for useful comments, which helped improve this review. I acknowledge the support from the Department of Science and Technology via SwaranaJayanti Fellowship award (file no. DST/SJF/PSA-01/2014-15). The chapter has benefitted immensely from discussions with Roger Chevalier, Claes Fransson, and Nikolai Chugai at various stages.

References

- Anderson JP, Habergham SM, James PA, Hamuy M (2012) Progenitor mass constraints for core-collapse supernovae from correlations with host galaxy star formation. *MNRAS* 424:1372–1391, DOI 10.1111/j.1365-2966.2012.21324.x, 1205.3802
- Bauer FE, Dwarkadas VV, Brandt WN, Immler S, Smartt S, Bartel N, Bietenholz MF (2008) Supernova 1996cr: SN 1987A’s Wild Cousin? *ApJ* 688:1210–1234, DOI 10.1086/589761, 0804.3597
- Bell AR (1978) The acceleration of cosmic rays in shock fronts. II. *MNRAS* 182:443–455, DOI 10.1093/mnras/182.3.443
- Bilinski C, Smith N, Li W, Williams GG, Zheng W, Filippenko AV (2015) Constraints on Type IIn supernova progenitor outbursts from the Lick Observatory Supernova Search. *MNRAS* 450:246–265, DOI 10.1093/mnras/stv566, 1503.04252
- Blandford RD, Ostriker JP (1978) Particle acceleration by astrophysical shocks. *ApJ Lett* 221:L29–L32, DOI 10.1086/182658
- Brown G, Bethe HA (1985) How a supernova explodes. *Scientific American* 252:60–68, DOI 10.1038/scientificamerican0585-60
- Chandra P, Chevalier RA (2017) Swift-XRT observations of Type IIn supernova ASASSN-17kr a.k.a. SN 2017gas. *The Astronomer’s Telegram* 10705
- Chandra P, Ray A, Bhatnagar S (2004) Synchrotron Aging and the Radio Spectrum of SN 1993J. *ApJ Lett* 604:L97–L100, DOI 10.1086/383615, astro-ph/0402391
- Chandra P, Ray A, Schlegel EM, Sutaria FK, Pietsch W (2005) Chandra’s Tryst with SN 1995N. *ApJ* 629:933–943, DOI 10.1086/431573, astro-ph/0505051
- Chandra P, Stockdale CJ, Chevalier RA, Van Dyk SD, Ray A, Kelley MT, Weiler KW, Panagia N, Sramek RA (2009) Eleven Years of Radio Monitoring of the type IIn Supernova SN 1995N. *ApJ* 690:1839–1846, DOI 10.1088/0004-637X/690/2/1839, 0809.2810
- Chandra P, Chevalier RA, Chugai N, Fransson C, Irwin CM, Soderberg AM, Chakraborti S, Immler S (2012a) Radio and X-Ray Observations of SN 2006jd: Another Strongly Interacting Type IIn Supernova. *ApJ* 755:110, DOI 10.1088/0004-637X/755/2/110, 1205.0250
- Chandra P, Chevalier RA, Irwin CM, Chugai N, Fransson C, Soderberg AM (2012b) Strong Evolution of X-Ray Absorption in the Type IIn Supernova SN 2010jl. *ApJ Lett* 750:L2, DOI 10.1088/2041-8205/750/1/L2, 1203.1614

-
- Chandra P, Chevalier RA, Chugai N, Fransson C, Soderberg AM (2015) X-Ray and Radio Emission from Type IIn Supernova SN 2010jl. *ApJ* 810:32, DOI 10.1088/0004-637X/810/1/32, 1507.06059
- Chevalier R, Blondin JM (1995) Hydrodynamic instabilities in supernova remnants: Early radiative cooling. *ApJ* 444:312–317, DOI 10.1086/175606
- Chevalier RA (1981) The interaction of the radiation from a Type II supernova with a circumstellar shell. *ApJ* 251:259–265, DOI 10.1086/159460
- Chevalier RA (1982a) Self-similar solutions for the interaction of stellar ejecta with an external medium. *ApJ* 258:790–797, DOI 10.1086/160126
- Chevalier RA (1982b) The radio and X-ray emission from type II supernovae. *ApJ* 259:302–310, DOI 10.1086/160167
- Chevalier RA (1998) Synchrotron Self-Absorption in Radio Supernovae. *ApJ* 499:810–819, DOI 10.1086/305676
- Chevalier RA (2012) Common Envelope Evolution Leading to Supernovae with Dense Interaction. *ApJ Lett* 752:L2, DOI 10.1088/2041-8205/752/1/L2, 1204.3300
- Chevalier RA, Fransson C (1994) Emission from circumstellar interaction in normal Type II supernovae. *ApJ* 420:268–285, DOI 10.1086/173557
- Chevalier RA, Fransson C (2003) Supernova Interaction with a Circumstellar Medium. In: Weiler K (ed) *Supernovae and Gamma-Ray Bursters, Lecture Notes in Physics*, Berlin Springer Verlag, vol 598, pp 171–194, [astro-ph/0110060](#)
- Chevalier RA, Fransson C (2016) Thermal and non-thermal emission from circumstellar interaction. *ArXiv e-prints* 1612.07459
- Chevalier RA, Irwin CM (2011) Shock Breakout in Dense Mass Loss: Luminous Supernovae. *ApJ Lett* 729:L6, DOI 10.1088/2041-8205/729/1/L6, 1101.1111
- Chugai NN (1990) Late Stage Radiation Source in Type-II Supernovae - Radioactivity or Shock Heating. *Soviet Astronomy Letters* 16:457
- Chugai NN, Chevalier RA (2006) Late Emission from the Type Ib/c SN 2001em: Overtaking the Hydrogen Envelope. *ApJ* 641:1051–1059, DOI 10.1086/500539, [astro-ph/0510362](#)
- Chugai NN, Danziger IJ (1994) Supernova 1988Z - Low-Mass Ejecta Colliding with the Clumpy Wind. *MNRAS* 268:173, DOI 10.1093/mnras/268.1.173
- Chugai NN, Danziger IJ (2003) A Massive Circumstellar Envelope around the Type-IIn Supernova SN 1995G. *Astronomy Letters* 29:649–657, DOI 10.1134/1.1615333, [astro-ph/0306330](#)
- Chugai NN, Blinnikov SI, Cumming RJ, Lundqvist P, Bragaglia A, Filippenko AV, Leonard DC, Matheson T, Sollerman J (2004) The Type IIn supernova 1994W: evidence for the explosive ejection of a circumstellar envelope. *MNRAS* 352:1213–1231, DOI 10.1111/j.1365-2966.2004.08011.x, [astro-ph/0405369](#)
- Cooke J, Sullivan M, Barton EJ, Bullock JS, Carlberg RG, Gal-Yam A, Tollerud E (2009) Type IIn supernovae at redshift $z \sim 2$ from archival data. *Nature* 460:237–239, DOI 10.1038/nature08082, 0907.1928
- Dilday B, Howell DA, Cenko SB, Silverman JM, Nugent PE, Sullivan M, Ben-Ami S, Bildsten L, Bolte M, Endl M, Filippenko AV, Gnat O, Horesh A, Hsiao E, Kasliwal MM, Kirkman D, Maguire K, Marcy GW, Moore K, Pan Y, Parrent JT, Podsiadlowski P, Quimby RM, Sternberg A, Suzuki N, Tytler DR, Xu D, Bloom JS, Gal-Yam A, Hook IM, Kulkarni SR, Law NM, Ofek EO, Polishook D, Poznanski D (2012) PTF 11kx: A Type Ia Supernova with a Symbiotic Nova Progenitor. *Science* 337:942, DOI 10.1126/science.1219164, 1207.1306
- Dwarkadas VV, Gruszko J (2012) What are published X-ray light curves telling us about young supernova expansion? *MNRAS* 419:1515–1524, DOI 10.1111/j.1365-2966.2011.19808.x, 1109.2616
- Dwarkadas VV, Romero-Cañizales C, Reddy R, Bauer FE (2016) X-ray and radio emission from the luminous supernova 2005kd. *MNRAS* 462:1101–1110, DOI 10.1093/mnras/stw1717, 1607.06104
- Fox OD, Van Dyk SD, Dwek E, Smith N, Filippenko AV, Andrews J, Arendt RG, Foley RJ, Kelly PL, Miller AA, Shivvers I (2017) The Candidate Progenitor of the Type IIn SN 2010jl Is Not an Optically Luminous Star. *ApJ* 836:222,

- DOI 10.3847/1538-4357/836/2/222, 1611.00369
- Fransson C (1984) Comptonization and UV emission lines from Type II supernovae. *A&A* 133:264–284
- Fransson C, Lundqvist P, Chevalier RA (1996) Circumstellar Interaction in SN 1993J. *ApJ* 461:993, DOI 10.1086/177119
- Fransson C, Ergon M, Challis PJ, Chevalier RA, France K, Kirshner RP, Marion GH, Milisavljevic D, Smith N, Bufano F, Friedman AS, Kangas T, Larsson J, Mattila S, Benetti S, Chornock R, Czekala I, Soderberg A, Sollerman J (2014) High-density Circumstellar Interaction in the Luminous Type II In SN 2010jl: The First 1100 Days. *ApJ* 797:118, DOI 10.1088/0004-637X/797/2/118, 1312.6617
- Fraser M, Inserra C, Jerkstrand A, Kotak R, Pignata G, Benetti S, Botticella MT, Bufano F, Childress M, Mattila S, Pastorello A, Smartt SJ, Turatto M, Yuan F, Anderson JP, Bayliss DDR, Bauer FE, Chen TW, Förster Burón F, Gal-Yam A, Haislip JB, Knapic C, Le Guillou L, Marchi S, Mazzali P, Molinaro M, Moore JP, Reichart D, Smareglia R, Smith KW, Sternberg A, Sullivan M, Takáts K, Tucker BE, Valenti S, Yaron O, Young DR, Zhou G (2013) SN 2009ip à la PESSTO: no evidence for core collapse yet. *MNRAS* 433:1312–1337, DOI 10.1093/mnras/stt813, 1303.3453
- Fullerton AW, Massa DL, Prinja RK (2006) The Discordance of Mass-Loss Estimates for Galactic O-Type Stars. *ApJ* 637:1025–1039, DOI 10.1086/498560, astro-ph/0510252
- Gal-Yam A, Leonard DC, Fox DB, Cenko SB, Soderberg AM, Moon DS, Sand DJ, Caltech Core Collapse Program, Li W, Filippenko AV, Aldering G, Copin Y (2007) On the Progenitor of SN 2005gl and the Nature of Type II In Supernovae. *ApJ* 656:372–381, DOI 10.1086/510523, astro-ph/0608029
- Hoffman JL, Leonard DC, Chornock R, Filippenko AV, Barth AJ, Matheson T (2008) The Dual-Axis Circumstellar Environment of the Type II In Supernova 1997eg. *ApJ* 688:1186–1209, DOI 10.1086/592261, 0709.3258
- Humphreys RM, Davidson K (1994) The luminous blue variables: Astrophysical geysers. *PASP* 106:1025–1051, DOI 10.1086/133478
- Humphreys RM, Davidson K, Smith N (1999) η Carinae's Second Eruption and the Light Curves of the η Carinae Variables. *PASP* 111:1124–1131, DOI 10.1086/316420
- Immler S (2007) X-Ray Emission from Supernovae. In: Immler S, Weiler K, McCray R (eds) *Supernova 1987A: 20 Years After: Supernovae and Gamma-Ray Bursters*, American Institute of Physics Conference Series, vol 937, pp 246–255, DOI 10.1063/1.3682910
- Katsuda S, Maeda K, Nozawa T, Pooley D, Immler S (2014) SN 2005ip: A Luminous Type II In Supernova Emerging from a Dense Circumstellar Medium as Revealed by X-Ray Observations. *ApJ* 780:184, DOI 10.1088/0004-637X/780/2/184, 1311.7180
- Katsuda S, Maeda K, Bamba A, Terada Y, Fukazawa Y, Kawabata K, Ohno M, Sugawara Y, Tsuboi Y, Immler S (2016) Two Distinct-absorption X-Ray Components from Type II In Supernovae: Evidence for Asphericity in the Circumstellar Medium. *ApJ* 832:194, DOI 10.3847/0004-637X/832/2/194, 1609.09093
- Leonard DC, Filippenko AV, Barth AJ, Matheson T (2000) Evidence for Asphericity in the Type II In Supernova SN 1998S. *ApJ* 536:239–254, DOI 10.1086/308910, astro-ph/9908040
- Li WD, Li C, Filippenko AV, Moran EC (1998) Supernova 1998S in NGC 3877. *IAU Circ* 6829
- Margutti R, Milisavljevic D, Soderberg AM, Guidorzi C, Morsony BJ, Sanders N, Chakraborti S, Ray A, Kamble A, Drout M, Parrent J, Zauderer A, Chomiuk L (2014) Relativistic Supernovae have Shorter-lived Central Engines or More Extended Progenitors: The Case of SN 2012ap. *ApJ* 797:107, DOI 10.1088/0004-637X/797/2/107, 1402.6344
- Margutti R, Kamble A, Milisavljevic D, Zapartas E, de Mink SE, Drout M, Chornock R, Risaliti G, Zauderer BA, Bietenholz M, Cantiello M, Chakraborti S, Chomiuk L, Fong W, Grefenstette B, Guidorzi C, Kirshner R, Parrent JT,

- Patnaude D, Soderberg AM, Gehrels NC, Harrison F (2017) Ejection of the Massive Hydrogen-rich Envelope Timed with the Collapse of the Stripped SN 2014C. *ApJ* 835:140, DOI 10.3847/1538-4357/835/2/140, **1601.06806**
- Matzner CD, McKee CF (1999) The Expulsion of Stellar Envelopes in Core-Collapse Supernovae. *ApJ* 510:379–403, DOI 10.1086/306571, **astro-ph/9807046**
- Mauerhan JC, Smith N, Filippenko AV, Blanchard KB, Blanchard PK, Casper CFE, Cenko SB, Clubb KI, Cohen DP, Fuller KL, Li GZ, Silverman JM (2013) The unprecedented 2012 outburst of SN 2009ip: a luminous blue variable star becomes a true supernova. *MNRAS* 430:1801–1810, DOI 10.1093/mnras/stt009, **1209.6320**
- McCray R, Fransson C (2016) The Remnant of Supernova 1987A. *ARA&A* 54:19–52, DOI 10.1146/annurev-astro-082615-105405
- Milisavljevic D, Margutti R, Kamble A, Patnaude DJ, Raymond JC, Eldridge JJ, Fong W, Bietenholz M, Challis P, Chornock R, Drout MR, Fransson C, Fesen RA, Grindlay JE, Kirshner RP, Lunnan R, Mackey J, Miller GF, Parrent JT, Sanders NE, Soderberg AM, Zauderer BA (2015) Metamorphosis of SN 2014C: Delayed Interaction between a Hydrogen Poor Core-collapse Supernova and a Nearby Circumstellar Shell. *ApJ* 815:120, DOI 10.1088/0004-637X/815/2/120, **1511.01907**
- Nymark TK, Fransson C, Kozma C (2006) X-ray emission from radiative shocks in type II supernovae. *A & A* 449:171–192, DOI 10.1051/0004-6361:20054169, **astro-ph/0510792**
- Ofek EO, Fox D, Cenko SB, Sullivan M, Gnat O, Frail DA, Horesh A, Corsi A, Quimby RM, Gehrels N, Kulkarni SR, Gal-Yam A, Nugent PE, Yaron O, Filippenko AV, Kasliwal MM, Bildsten L, Bloom JS, Poznanski D, Arcavi I, Laher RR, Levitan D, Sesar B, Surace J (2013) X-Ray Emission from Supernovae in Dense Circumstellar Matter Environments: A Search for Collisionless Shocks. *ApJ* 763:42, DOI 10.1088/0004-637X/763/1/42, **1206.0748**
- Ofek EO, Sullivan M, Shaviv NJ, Steinbok A, Arcavi I, Gal-Yam A, Tal D, Kulkarni SR, Nugent PE, Ben-Ami S, Kasliwal MM, Cenko SB, Laher R, Surace J, Bloom JS, Filippenko AV, Silverman JM, Yaron O (2014a) Precursors Prior to Type II_n Supernova Explosions are Common: Precursor Rates, Properties, and Correlations. *ApJ* 789:104, DOI 10.1088/0004-637X/789/2/104, **1401.5468**
- Ofek EO, Zoglauer A, Boggs SE, Barrière NM, Reynolds SP, Fryer CL, Harrison FA, Cenko SB, Kulkarni SR, Gal-Yam A, Arcavi I, Bellm E, Bloom JS, Christensen F, Craig WW, Even W, Filippenko AV, Grefenstette B, Hailey CJ, Laher R, Madsen K, Nakar E, Nugent PE, Stern D, Sullivan M, Surace J, Zhang WW (2014b) SN 2010jl: Optical to Hard X-Ray Observations Reveal an Explosion Embedded in a Ten Solar Mass Cocoon. *ApJ* 781:42, DOI 10.1088/0004-637X/781/1/42, **1307.2247**
- Pacholczyk AG (1970) Radio astrophysics. Nonthermal processes in galactic and extragalactic sources. Series of Books in Astronomy and Astrophysics, San Francisco: Freeman, 1970
- Panagia N, Felli M (1975) The spectrum of the free-free radiation from extended envelopes. *A&A* 39:1–5
- Pastorello A, Smartt SJ, Mattila S, Eldridge JJ, Young D, Itagaki K, Yamaoka H, Navasardyan H, Valenti S, Patat F, Agnoletto I, Augusteijn T, Benetti S, Cappellaro E, Boles T, Bonnet-Bidaud JM, Botticella MT, Bufano F, Cao C, Deng J, Dennefeld M, Elias-Rosa N, Harutyunyan A, Keenan FP, Iijima T, Lorenzi V, Mazzali PA, Meng X, Nakano S, Nielsen TB, Smoker JV, Stanishev V, Turatto M, Xu D, Zampieri L (2007) A giant outburst two years before the core-collapse of a massive star. *Nature* 447:829–832, DOI 10.1038/nature05825, **astro-ph/0703663**
- Patat F, Taubenberger S, Benetti S, Pastorello A, Harutyunyan A (2011) Asymmetries in the type II_n SN 2010jl. *A&A* 527:L6, DOI 10.1051/0004-6361/201016217, **1011.5926**
- Perez-Torres M, Alberdi A, Beswick RJ, Lundqvist P, Herrero-Illana R, Romero-Cañizales C, Ryder S, della Valle M, Conway J, Marcaide JM, Mattila S, Mur-

- phy T, Ros E (2015) Core-collapse and Type Ia supernovae with the SKA. *Advancing Astrophysics with the Square Kilometre Array (AASKA14)* 60, 1409.1827
- Puls J, Vink JS, Najarro F (2008) Mass loss from hot massive stars. *A&ARv* 16:209–325, DOI 10.1007/s00159-008-0015-8, 0811.0487
- Quataert E, Shiode J (2012) Wave-driven mass loss in the last year of stellar evolution: setting the stage for the most luminous core-collapse supernovae. *MNRAS* 423:L92–L96, DOI 10.1111/j.1745-3933.2012.01264.x, 1202.5036
- Quimby RM, Yuan F, Akerlof C, Wheeler JC (2013) Rates of superluminous supernovae at $z \sim 0.2$. *MNRAS* 431:912–922, DOI 10.1093/mnras/stt213, 1302.0911
- Ross M, Dwarkadas VV (2017) SNaX - A Database of Supernova X-ray Lightcurves. *ArXiv e-prints* 1704.05866
- Salamanca I, Cid-Fernandes R, Tenorio-Tagle G, Telles E, Terlevich RJ, Munoz-Tunon C (1998) The circumstellar medium of the peculiar supernova SN1997ab. *MNRAS* 300:L17–L21, DOI 10.1046/j.1365-8711.1998.02093.x, astro-ph/9809208
- Sanders NE, Soderberg AM, Foley RJ, Chornock R, Milisavljevic D, Margutti R, Drout MR, Moe M, Berger E, Brown WR, Lunnan R, Smartt SJ, Fraser M, Kotak R, Magill L, Smith KW, Wright D, Huang K, Urata Y, Mulchaey JS, Rest A, Sand DJ, Chomiuk L, Friedman AS, Kirshner RP, Marion GH, Tonry JL, Burgett WS, Chambers KC, Hodapp KW, Kudritzki RP, Price PA (2013) PS1-12sk is a Peculiar Supernova from a He-rich Progenitor System in a Brightest Cluster Galaxy Environment. *ApJ* 769:39, DOI 10.1088/0004-637X/769/1/39, 1303.1818
- Schlegel EM, Petre R (2006) A Chandra ACIS Observation of the X-Ray-luminous SN 1988Z. *ApJ* 646:378–384, DOI 10.1086/504890, astro-ph/0604106
- Schlegel EM, Kong A, Kaaret P, DiStefano R, Murray S (2004) Chandra ACIS and XMM-Newton EPIC Observations of the X-Ray-Luminous SN 1978K in NGC 1313. *ApJ* 603:644–651, DOI 10.1086/381571, astro-ph/0311434
- Smith N (2010) Episodic post-shock dust formation in the colliding winds of Eta Carinae. *MNRAS* 402:145–151, DOI 10.1111/j.1365-2966.2009.15901.x, 0910.4395
- Smith N (2014) Mass Loss: Its Effect on the Evolution and Fate of High-Mass Stars. *ARA&A* 52:487–528, DOI 10.1146/annurev-astro-081913-040025, 1402.1237
- Smith N (2016) Interacting Supernovae: Types IIn and Ibn. *ArXiv e-prints* 1612.02006
- Smith N, Tombleson R (2015) Luminous blue variables are antisocial: their isolation implies that they are kicked mass gainers in binary evolution. *MNRAS* 447:598–617, DOI 10.1093/mnras/stu2430, 1406.7431
- Smith N, Hinkle KH, Ryde N (2009) Red Supergiants as Potential Type IIn Supernova Progenitors: Spatially Resolved 4.6 μm CO Emission Around VY CMa and Betelgeuse. *AJ* 137:3558–3573, DOI 10.1088/0004-6256/137/3/3558, 0811.3037
- Smith N, Chornock R, Silverman JM, Filippenko AV, Foley RJ (2010) Spectral Evolution of the Extraordinary Type IIn Supernova 2006gy. *ApJ* 709:856–883, DOI 10.1088/0004-637X/709/2/856, 0906.2200
- Smith N, Li W, Miller AA, Silverman JM, Filippenko AV, Cuillandre JC, Cooper MC, Matheson T, Van Dyk SD (2011) A Massive Progenitor of the Luminous Type IIn Supernova 2010jl. *ApJ* 732:63, DOI 10.1088/0004-637X/732/2/63, 1011.4150
- Smith N, Silverman JM, Filippenko AV, Cooper MC, Matheson T, Bian F, Weiner BJ, Comerford JM (2012) Systematic Blueshift of Line Profiles in the Type IIn Supernova 2010jl: Evidence for Post-shock Dust Formation? *AJ* 143:17, DOI 10.1088/0004-6256/143/1/17, 1108.2869
- Smith N, Andrews JE, Mauerhan JC (2016) Massive stars dying alone: the extremely remote environment of SN 2009ip. *MNRAS* 463:2904–2911, DOI 10.1093/mnras/stw2190, 1607.01056
- Sollerman J, Cumming RJ, Lundqvist P (1998) A Very Low Mass of ^{56}Ni in the Ejecta of SN 1994W. *ApJ* 493:933–939, DOI 10.1086/305163, astro-ph/9709061

-
- Svirski G, Nakar E, Sari R (2012) Optical to X-Ray Supernova Light Curves Following Shock Breakout through a Thick Wind. *ApJ* 759:108, DOI 10.1088/0004-637X/759/2/108, 1202.3437
- Temple RF, Raychaudhury S, Stevens IR (2005) X-ray observations of the edge-on star-forming galaxy NGC 891 and its supernova SN1986J. *MNRAS* 362:581–591, DOI 10.1111/j.1365-2966.2005.09336.x, [astro-ph/0506657](#)
- Turatto M, Cappellaro E, Danziger IJ, Benetti S, Gouiffes C, della Valle M (1993) The Type II supernova 1988Z in MCG + 03-28-022 - Increasing evidence of interaction of supernova ejecta with a circumstellar wind. *MNRAS* 262:128–140, DOI 10.1093/mnras/262.1.128
- van Dyk SD, Weiler KW, Sramek RA, Panagia N (1993) SN 1988Z: The Most Distant Radio Supernova. *ApJ Lett* 419:L69, DOI 10.1086/187139
- van Dyk SD, Weiler KW, Sramek RA, Schlegel EM, Filippenko AV, Panagia N, Leibundgut B (1996) Type “II_n” Supernovae: A Search for Radio Emission. *AJ* 111:1271, DOI 10.1086/117872
- Vink JS, de Koter A, Lamers HJGLM (2001) Mass-loss predictions for O and B stars as a function of metallicity. *A&A* 369:574–588, DOI 10.1051/0004-6361:20010127, [astro-ph/0101509](#)
- Wang L, Cui X, Zhu H, Tian W (2015) Investigations of supernovae and supernova remnants in the era of SKA. *Advancing Astrophysics with the Square Kilometre Array (AASKA14)* 64, 1501.04645
- Weiler KW, Panagia N, Sramek RA (1990) Radio emission from supernovae. II - SN 1986J: A different kind of type II. *ApJ* 364:611–625, DOI 10.1086/169444
- Weiler KW, Panagia N, Montes MJ, Sramek RA (2002) Radio Emission from Supernovae and Gamma-Ray Bursters. *ARA&A* 40:387–438, DOI 10.1146/annurev.astro.40.060401.093744
- Williams CL, Panagia N, Van Dyk SD, Lacey CK, Weiler KW, Sramek RA (2002) Radio Emission from SN 1988Z and Very Massive Star Evolution. *ApJ* 581:396–403, DOI 10.1086/344087, [astro-ph/0208190](#)
- Woosley SE, Blinnikov S, Heger A (2007) Pulsational pair instability as an explanation for the most luminous supernovae. *Nature* 450:390–392, DOI 10.1038/nature06333, 0710.3314